

*Review paper*

# **Paving the Way to the Integration of Smart Nanostructures: Part 1: Nanotethering and Nanowiring via Material Nanoengineering and Electrochemical Identification.**

Michael E.G. Lyons<sup>1,\*</sup>, Serge Rebouillat<sup>2,\*\*</sup>

<sup>1</sup> Physical and Materials Electrochemistry Laboratory, School of Chemistry, University of Dublin, Trinity College, Dublin 2, Ireland

<sup>2</sup> DuPont International S.A., 2 chemin du Pavillon, CH1218 Le Grand Saconnex, Geneva, Switzerland

\*E-mail: [melyons@tcd.ie](mailto:melyons@tcd.ie)

\*\*E-mail: [serge.rebouillat@che.dupont.com](mailto:serge.rebouillat@che.dupont.com)

*Received:* 22 February 2009 / *Accepted:* 13 March 2009 / *Published:* 22 March 2009

---

In this review essay some recent approaches to nanotethering and nanowiring of biomolecules such as redox enzymes and nanoparticles to solid surfaces to generate chemically modified electrodes to serve as platforms for bottom up designed nanostructures for use in nanobioelectronics are described.

---

**Keywords:** amperometric enzyme electrodes, electrochemical glucose detection, monolayer protected metal nanoparticles, carbon nanotube electrochemistry

## **1. INTRODUCTION**

The advances in human lifestyle of the last century are to a great extent attributable to the fruits of science and technology. Medical, communication and materials advances have all been dramatic, and the assumption that there will be more progress is now built into our whole economic and social thinking. A key driver is control of matter at ever decreasing scales. This is obvious in data storage and integrated circuits, but is also true in biology (single molecule medicine) and in new materials and sensors. Observation, analysis, and control of structures at the atomic, molecular and sub-micron scale, defines the new frontier of nanotechnology. Hence it is not unreasonable to assert that the science and technology of the 21<sup>st</sup> century will be driven by the direct manipulation of events at the atomic or molecular level. The nanometer length scale will define 21<sup>st</sup> century scientific endeavor. At a billionth or one thousand millionth ( $10^{-9}$ ) of a meter, a nanometer is the essence of small. The width of 10 hydrogen atoms laid side by side, it is one thousandth the length of a typical bacterium, one millionth

the size of a pinhead, and one billionth the size of a human. A single human hair is about 80,000 nm wide, a red blood cell about 7000 nm wide and a water molecule is almost 0.3 nm across. The nanoworld defines the border zone between the realm of individual atoms and molecules (where quantum mechanics rules), and the macroworld, where the bulk properties of materials emerge from the collective behavior of atoms.

There are important reasons for the current focus on nanotechnology. Powerful new tools with wide application, such as scanned probe microscopes and ultrafine sample preparation methods, have recently become available to work reliably at that scale. Complex nanosystems are now amenable to accurate computational simulation, enhancing our understanding of their function and adaptability. The interface between biological systems and inorganic devices is particularly fruitful at the nanoscale, with great potential for medical analysis and bio-synthesis - this is typical of the key role of interdisciplinarity in nanoscience. Finally, the nanoscale is the frontier of the continued scaling of IT devices and the likely source of radically new functions. This is where new, and sometimes unexpected discoveries, of potential technical value, will be made - serendipity in science is as significant as targeted technology support. It is not surprising that almost all industrialized nations have initiated and funded substantial nanoscience and technology programmes and considerable information of high value may be obtained from the web [1-5].

One of the grand challenges facing science in the 21<sup>st</sup> century is to develop well defined smart structures of nanometer dimension. Fundamental progress has already been made in a number of important areas underlying smart nanostructure fabrication, such as the fundamental understanding of the physicochemical properties of nanostructures, the synthesis of nanoscale materials, the imaging of nanostructures and the assembly of functional nanoscale devices. In the present paper some examples of the latter 'smart nanostructures' will be discussed. The examples presented will, of necessity, reflect the expertise and interests of the authors, and will be concerned with the positive impact that materials and physical chemistry can make in nanobiotechnology.

Specifically, the properties of nanometer-sized particles [6] and nanostructured thin films [7] are of intense contemporary interest, driven by both fundamental questions and possibilities for use in nanoscale technology. As recently noted by Drechsler and co-workers [6d], nanoparticles and organized nanostructured films provide a means of bridging the gap between 'top down' lithographic techniques [4a] and 'bottom up' synthetic strategies [8b] as well as a versatile scaffold for the introduction of specific chemical functionality [6b,8c]. The vexed question of linking useful nanostructures to surfaces as part of device construction is also a topic of intense current interest and activity. The concept of molecular 'wiring' using single walled carbon nanotubes (SWCNT) [9,10] has proved to be useful in this context.

In the following sections we explore the potential afforded by self assembled nanostructures<sup>1</sup> as components in smart integrated systems. In particular attention is focused on the interfacial, redox and catalytic properties of polycrystalline metals coated with alkanethiol based organic thin films and metal nanoclusters coated with an alkane thiol shell. For both types of systems the organic monolayer

---

<sup>1</sup> Self assembly is a spontaneous coordinated action of independent entities to produce a larger structure. The concept finds application in biology (embryology and morphogenesis) and chemistry (the formation of supramolecular structures from small molecules).

film/ shell serves as a well organized scaffold for the attachment of functional molecular units which can exhibit both molecular recognition and catalytic properties (fig.1(a)). We will show how electrochemical methodology can be used to probe the dynamic properties of these systems. Attention will also focus on describing recent efforts on developing strategies involving the efficient wiring of useful biological nanostructures such as redox proteins and enzymes to surfaces using ordered arrays of single walled carbon nanotubes (SWCNT) (fig.1(b)). In this way smart integrated nanostructures may be constructed ‘to order’.

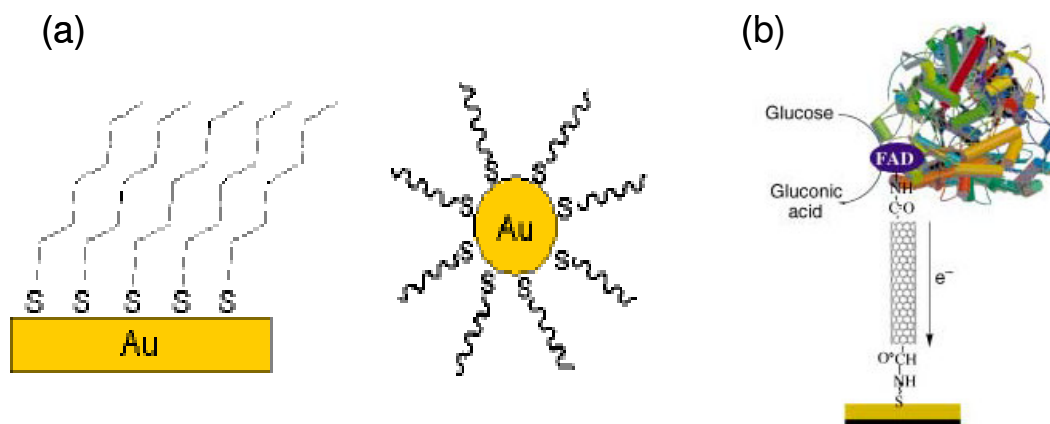


**Figure 1.** (a) Schematic representation of Self Assembled Monolayer (SAM) (left) and Monolayer Protected Metal Nanocluster (MPNC) (right) of alkane thiol molecules on gold substrate surface and nanoparticle. (b) Schematic representation of single walled carbon nanotube acting as a nanowire for connection of redox protein to a metal surface.

## 2. SELF ASSEMBLED NANOSTRUCTURED THIN FILM ASSEMBLIES

An organized SAM consists of a single layer of molecules on a substrate in which the molecules exhibit a high degree of orientation, molecular order and packing (fig.1(a)). The inherent order associated with self-assembled monolayers (SAMs) in particular accords them the potential to act as a support matrix in which individual molecules and more complex nanostructures can be isolated and addressed. In self assembly the monolayer spontaneously forms upon exposure of the substrate surface (such as gold) to a dilute solution or vapour containing, for example, sulfur containing (thiol, disulfide and sulfide) molecules. The sulfur compounds most commonly contain pendant alkane chains of varying length (see fig.2(a) below), but can also contain hetero atoms, aromatic groups, and conjugated unsaturated links. The latter are used particularly in molecular wire applications.

The initial molecular adsorption process is rapid and is essentially complete within minutes. The subsequent self assembly process is very slow, at least for the situation of passive self assembly (see fig.2(b) below). If the adsorption /self assembly experiment is performed under electrochemical control, the resultant SAM film is formed over a much shorter timescale with excellent reproducibility, and is of better quality than that formed via the passive incubation method [11,12]. Adsorption and

self assembly of alkane thiol monolayer films are also effected significantly by the presence of external magnetic fields [13].

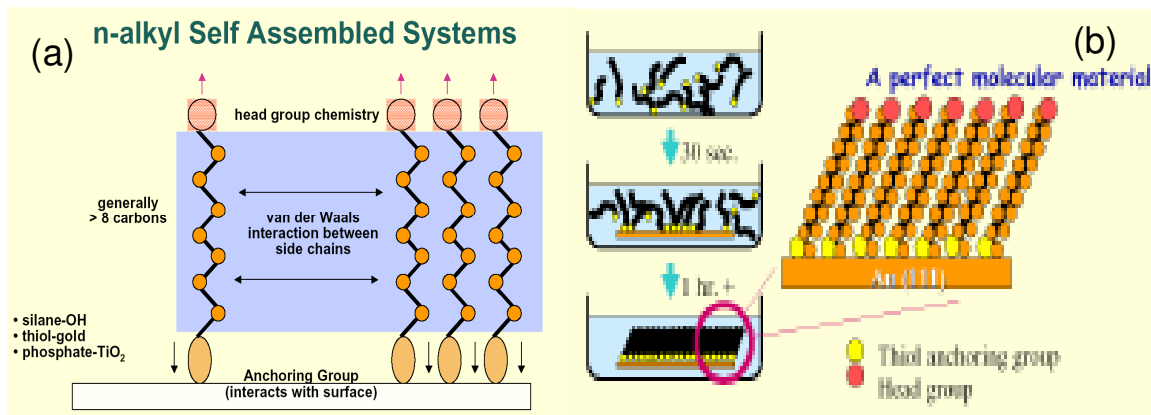


**Figure 2.** (a) Schematic representation of major factors influencing stability of self assembled monolayer. (b) Details of protocol required for passive SAM preparation.

Successful self assembly requires a relatively strong bond between the substrate and an atom or a moiety in the molecule (the anchor group) and an additional lateral interaction between molecules in the monolayer. The physicochemical properties and ultimate application of the SAM will be defined in many cases by the particular identity of the head group. The nature of the head group may be controlled by suitable synthetic design. In particular the head group may be electroactive and therefore capable of undergoing oxidation or reduction. This feature ensures that the redox properties of an electroactive SAM may be probed in real time using a variety of transient electrochemical techniques such as cyclic voltammetry and potential step chronoamperometry.

Mixed monolayer systems containing both redox active and analogous electroinactive structures which serve as diluents can be readily prepared by depositing different molecules simultaneously or sequentially. When both molecules are present in the deposition solution, the mole fraction of each molecular component in the SAM can be controlled via the fixing of the mole ratio of the components in the solution, and will also depend on the identity of the solvent, the solution temperature and the deposition time. The distribution of the two molecular components may vary from intimately mixed to completely phase separated. In sequential deposition, a second component is incorporated, via place exchange, into an existing SAM by prolonged immersion of the substrate in the second deposition solution. Hence, in principle, a surface confined redox species can be diluted in a controlled manner to generate an array in which the redox sites are far enough apart so that they do not interact with one another. The application of well established electrochemical techniques to the latter system offers the ability to answer many thermodynamic, kinetic and structural questions relevant to the construction of molecular electronic and nanobiotechnology based devices.

In electrochemical studies, the utility of thiol based SAMs arises from their ability to survive the electrochemical experiment. The sulfur atoms resist oxidation, reduction and desorption. SAMs on electrodes are stable over a wide range of potentials and electrolyte compositions (especially aqueous

electrolyte solutions). They afford a means of controlling the electrode-electrolyte interfacial properties and the accessibility of the electrode surface to solution phase molecules. SAMs also provide a means for fabricating a large range of chemically modified electrodes, ranging from modified monolayers to complex multilayers containing catalytic/receptor components. Specific applications include the development of more sensitive and selective electrochemical sensors (especially biosensors<sup>2</sup>), and the control of Faradaic electron transfer processes over long distances and at large driving forces.

For example, at present, the technology for the assembly of single molecules and other nanoscale components into robust and reproducible two and three terminal devices is still in its infancy, and represents one of the major 'grand challenges' of this area, and involves the measurement, understanding, and ultimate control of, charge transport at nanoscale and molecular contacts, and across thin films [14]. Indeed, thorough and quantitative studies of electron transfer in single molecule device structures remains extremely difficult. Smart structures based on self assembled monolayer (SAM systems) deposited on inert metallic support surfaces serve as ideal platforms to surmount the latter challenge of understanding nanoscale transport [15]. Hence the tethering of molecules to noble metal surfaces has been the subject of intense investigation over the past few years because of their potential for use in the technologies underpinning ICT and biotechnology. SAM nanostructures also provide, for example, an excellent test bed for examining the dynamics of long range electron transfer through organic bridges [16] (a key element in molecular electronics) and can act as units to anchor complex biological molecules such as proteins to electrode surfaces and thus enable the direct study of ET events involving redox active sites and support electrode surfaces (a process which underpins, and currently limits, biosensor operation) [17-19]. Consequently the attainment of a sound fundamental understanding of these systems will convey considerable benefit for future technological exploitation.

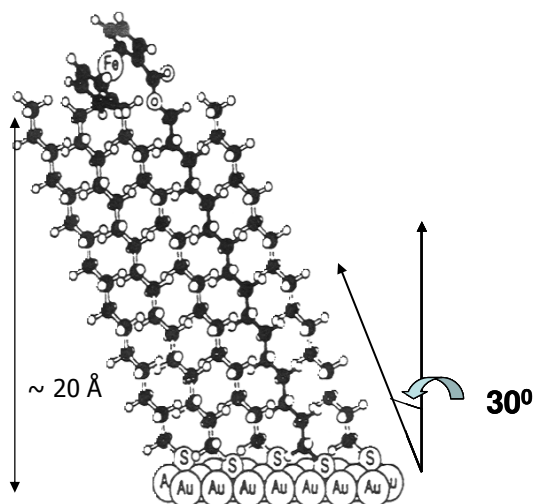


**Figure 3.** Schematic representation of mixed monolayer containing redox active and inactive alkane thiol chains. The redox active head group is ferrocene.

<sup>2</sup> A biosensor is defined as a sensing device consisting of a biological recognition element in intimate contact with a suitable transducer, which is able to convert the biological recognition reaction or eventually the biocatalytic process into a measurable electronic signal.

Redox active ferrocenylcarbonyloxy alkane thiols of various hydrocarbon chain lengths (C6-C12) can be readily prepared in high yield via reasonably simple synthetic pathways. These can be self assembled at open circuit (or indeed under anodic polarization conditions), on gold support electrodes (the latter in contact with a dilute (0.1  $\mu$ M-1mM) ethanolic solution of the alkane thiol ) to form redox active well ordered monolayer thin films. The redox behaviour of the latter is based on the ferrocene/ferricinium redox couple which is well behaved, and is used extensively as a benchmark system in electrochemical studies. The redox chemistry of the surface immobilized monolayer film can be followed in real time using a combination of cyclic voltammetry and the electrochemical quartz crystal microbalance [20].<sup>3</sup> Using the latter combination of techniques both changes in the redox composition of the layer as well as ion ingress/egress may be monitored.

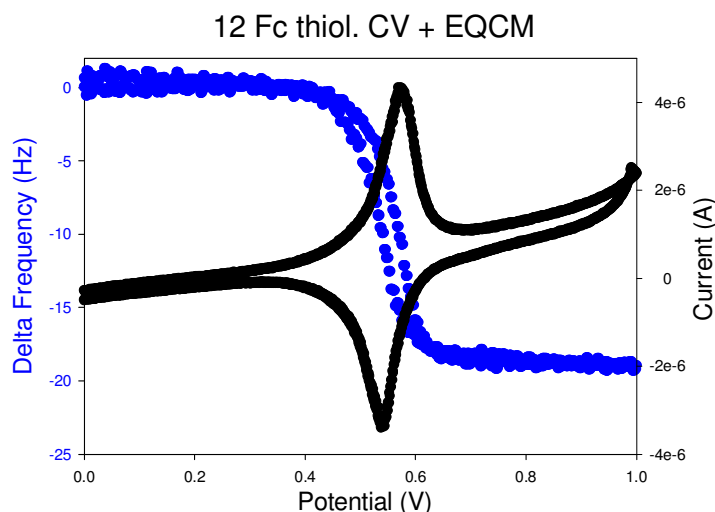


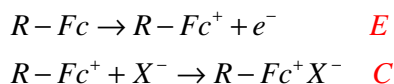
**Figure 4.** Typical CV and EQCM data recorded for 12-(Ferrocenylcarbonyloxy)dodecyl Thiol SAM in 0.1 M HClO<sub>4</sub> solution.

Typical voltammetric and gravimetric data obtained for a SAM comprising of 12-(Ferrocenylcarbonyloxy)dodecyl Thiol units in aqueous HClO<sub>4</sub> is outlined in figure 4 above. The peak

<sup>3</sup> The quartz crystal microbalance (QCM) is a variant of acoustic wave microsensors that are capable of ultrasensitive mass measurements. Under favourable conditions a typical QCM can measure a mass change of 0.1-1 ng/cm<sup>2</sup>. The QCM oscillates in a mechanically resonant shear mode (determined by the dimensions of the crystal and the mass loading) under the influence of a high frequency AC electric field which is applied across the thickness of the crystal. A change in the mass of the substrate electrode causes a change in the value of the resonant frequency of the piezoelectric device which can then be related directly to the quantity of added mass via the Sauerbrey equation:  $\Delta f = -C_f \Delta m = -\frac{2f_0^2}{\sqrt{\rho\mu A}} \Delta m$  where

$C_f$  is a constant which depends on the density  $\rho$  of the quartz crystal,  $\mu$  the shear modulus of the quartz, the area  $A$  of the gold coated quartz disc and  $f_0$  the resonant frequency of the fundamental mode of the crystal. Hence an increase in mass implies a decrease in frequency, and one can use small changes in frequency to monitor very small changes in mass in a very accurate manner. In the EQCM setup used in the author's laboratory a  $\Delta f$  value of 1 Hz corresponds to a  $\Delta m$  value of 1.4 ng.

observed on the forward oxidative potential sweep, is associated with the ferrocene/ferricinium redox reaction and a coupled ion transfer/binding process involving  $\text{ClO}_4^-$  ion ingress from the solution phase. Hence the reaction sequence may be labeled as an EC process (E : redox ET, C : ion pair formation). The reverse sequence (ferricinium/ferrocene, perchlorate ion egress to solution from SAM) occurs on reductive sweep. The EC mechanism can be represented as follows:



The latter coupled ET/ion transfer /ion pair formation processes may be illustrated schematically in figure 5 below. The decrease in frequency measured via the gravimetric EQCM experiment (presented in fig.4) during oxidative redox switching is  $\Delta f = 18.5 \text{ Hz}$  which corresponds to a mass increase of ca.  $2.5 \times 10^{-8} \text{ g}$ . The latter is approximately equivalent to one perchlorate ion per ferricinium redox site being incorporated into the SAM film during the oxidative potential sweep. The experiment illustrates the manner in which electrochemical measurements can be used to probe the stoichiometry of surface redox processes to a very high resolution. The redox switching process involving coupled electron transfer and ion pair formation is presented schematically in fig.5 below.

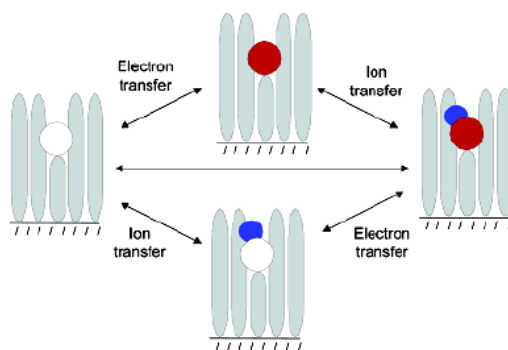


**Figure 5.** Schematic representation redox switching in SAM thin films. White circle represents reduced redox group, red circle represents oxidized redox group. Blue circle corresponds to charge compensating counterion species.

It has been established that redox switching of ferrocenylalkanethiols thin films deposited on electrode surfaces is accompanied by structural reorientation associated with ferrocene group rotation. The manner in which the voltammetric profile varies with experimental timescale, change in oxidation state and electrolyte concentration can be rationalized in terms of double layer effects [21,22], although a fully comprehensive theoretical understanding of the SAM/aqueous solution interface is still outstanding [23].

Enzyme molecules may be immobilized on electrode surfaces to form smart bio-electrocatalytic nanostructures using thiol molecules as a molecular ‘glue’ [17(d)] as illustrated in fig.6. The controlled covalent linkage of redox proteins and enzymes to electrode surface is a very effective and attractive strategy for the ‘bottom up’ fabrication of tailor made biosensor devices. For

example amino- or carboxylic acid functionalized thiolate monolayers associated with gold electrode surfaces can be coupled to complementary carboxylic or amino groups of glutamic, aspartic or lysine residues of enzymes and redox proteins. This concept utilizes functional group coupling chemistry at a solid surface. A wide variety of redox active biomolecules have been attached to electrode surfaces using this technique including glucose oxidase, glucose dehydrogenase, bilirubin oxidase, diphorase, glutathione reductase, microperoxidase 11, catalase and choline oxidase.

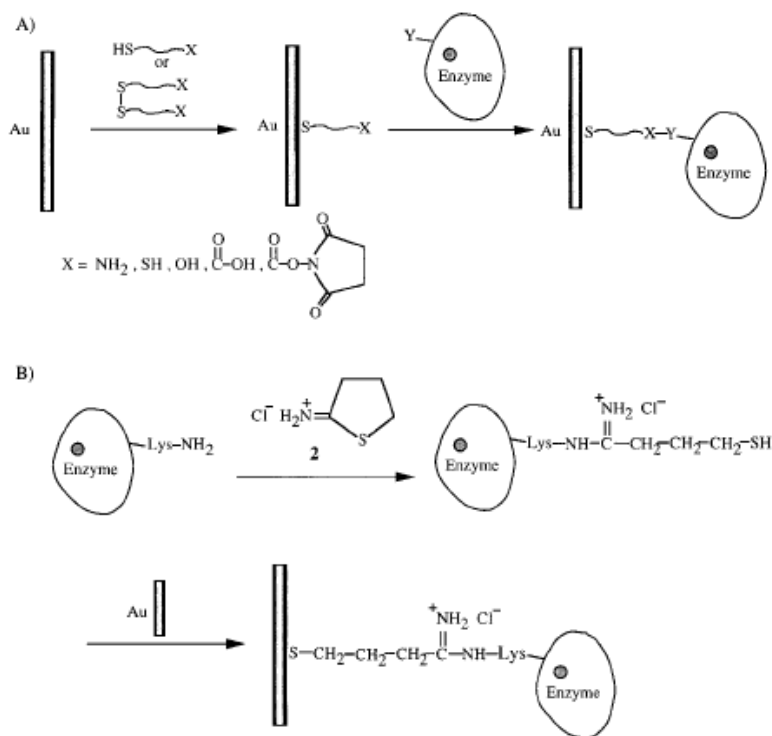


**Figure 6.** (A) Self assembly of functionalized thiolated monolayers on Au electrodes for the covalent linkage of enzymes. X denotes a functional group for coupling with a protein. Y represents a complementary functional group to X. (B) Modification of proteins with thiol functionalities for self assembly on Au supports. (Adapted from reference 17d).

It should be noted that the direct modification of solid supports by proteins is often associated with the denaturation of the latter in the primary adsorbate layer on the surface. However (fig.6(B)) chemical modification of the lysine residues present on the surface of the protein molecule with thiol tethers allows the selective association of the thiol groups to the gold support without denaturation of the protein taking place. It is easy to see that an enzyme base layer associated with a conductive support can be used as an active interface for the stepwise construction of three dimensional multilayer protein arrays [24,25]. This idea is illustrated schematically in fig.7 below.

In this approach enzymes are directly assembled in a controlled manner via covalent bonding onto an electrode surface. Furthermore electrical contact between the redox protein and the electrode surface is enhanced by chemical modification of the protein sheath (redox wiring) using an electron transfer relay compound (in this case a substituted ferrocene species). The effectiveness of the

electronic communication between the active site of the enzyme which is the FAD/FADH<sub>2</sub> group in the case of GOx and the support electrode surface is controlled by the tether length linking the redox mediator to the protein. The effectiveness of the ferrocene mediator will depend on the flexibility of the tether chain. As noted in fig.8 the tethered ferrocene species acts as an electronic stepping stone which facilitates the transfer of charge from the site of redox/catalytic activity to the support electrode surface.

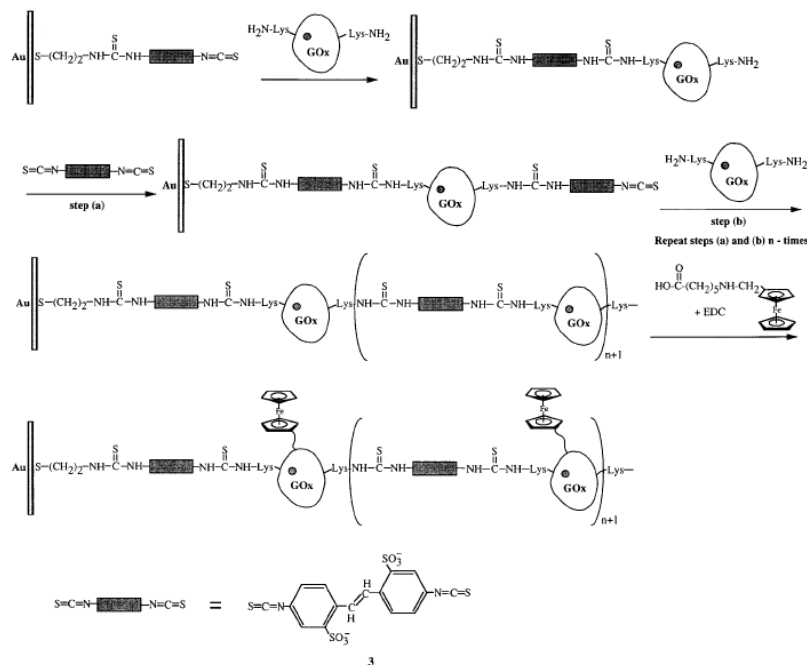


**Figure 7.** Stepwise assembly and electrical wiring of a cross linked multilayer array of Glucose Oxidase on a gold support electrode.(Adapted from reference 25).

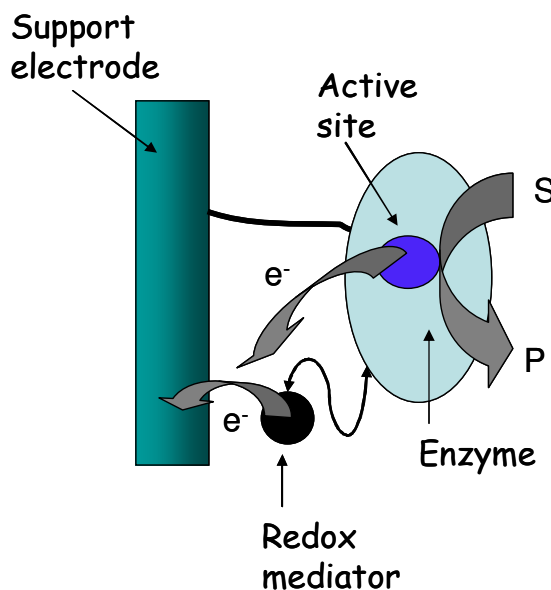


**Figure 8.** Redox wiring of a redox active enzyme such as glucose oxidase (GOx) by a tethered small molecule redox mediator (e.g. a modified ferrocene species).

It is possible to control the surface coverage of enzyme to a constant value (typically  $10^{-11}$  mol  $\text{cm}^{-2}$ ), within each slice of the multilayered structure. Up to 12 layers of enzyme have been assembled using this sequential method, and it has been noted that the amperometric sensor current increases with increasing number of enzyme layers. Riklin and Willner (25) have shown that a four layer GOx network electrode exhibits a good sensitivity and dynamic response for glucose detection (5-20 mM) when a potential of 0.4 V is applied in phosphate buffer solution pH 7.3 as illustrated in fig.9. The shape of the calibration curve is characteristic of Michaelis-Menten enzyme kinetics and can be fitted to a rectangular hyperbola using the expression:  $i_{ss} = \frac{i_m c}{K_M + c}$  where  $i_m$  denotes the maximum steady state amperometric current which is in turn related to the catalytic rate constant  $k_{cat}$  for the redox enzyme, and  $K_M$  denotes the Michaelis constant for the enzyme. We note from figure 9(A) that the fit is reasonable (correlation coefficient = 0.981) and non linear least squares fitting of the reported [25] batch amperometric data suggests that  $i_m = 1359 \pm 123 \mu\text{A}$  and  $K_M = 6.14 \pm 1.48 \text{ mM}$ . The data can be analyzed via a linear transformation of the Michaelis-Menten equation to a double reciprocal Lineweaver-Burk formulation as presented in fig.9(B), but it is more accurate and consequentially preferable to fit the kinetic expression directly to the raw data. In summary, it is reasonable to suggest the operation of effective electronic communication between the ferrocene mediator units and the support electrode exists and also that the bimolecular reaction kinetics between the mediator and the active site in the enzyme is rapid. These layered GOx electrodes may be stored dry at 4°C for periods of up to 6 months without losing catalytic activity. They also exhibit a stable response for at least 12 hours when operated amperometrically in solution. Hence they are particularly robust, and may offer potential as practical glucose biosensor devices.

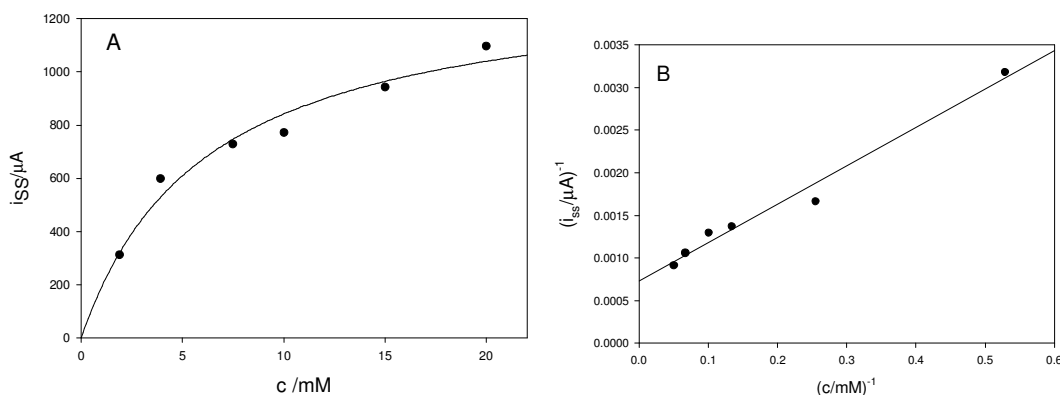


**Figure 9.** (a) Calibration curve illustrating amperometric current response at 0.4 V for 4 layer GOx electrode in phosphate buffer solution pH 7.3. (b) Lineweaver-Burk analysis of batch amperometric data presented in fig. 9(a).

It is possible to adapt the methodology to fabricate multilayer structures consisting of two distinct enzymes (choline oxidase and acetylcholine esterase [25]). This in principle is a very fruitful development since it enables a structured biosensing device based on enzyme amplification to be fabricated from the bottom up.

The concept of enzyme amplification is illustrated schematically in fig.10. Here two enzymes may be coupled together in a multilayered configuration. Thus a primary and a secondary enzyme is used. The product  $P_1$  of the secondary enzymatic reaction serves as the substrate  $S_2$  for the primary enzymatic reaction. Note that the secondary enzyme may well be electroinactive. The surface of the primary electroactive enzyme  $E_2$  may be modified with a charge transfer mediator  $R$  to facilitate charge transfer to the support electrode surface. The idea will only work effectively if the product formed by the secondary enzyme does not escape rapidly into the bulk solution before it can react with the primary enzyme.

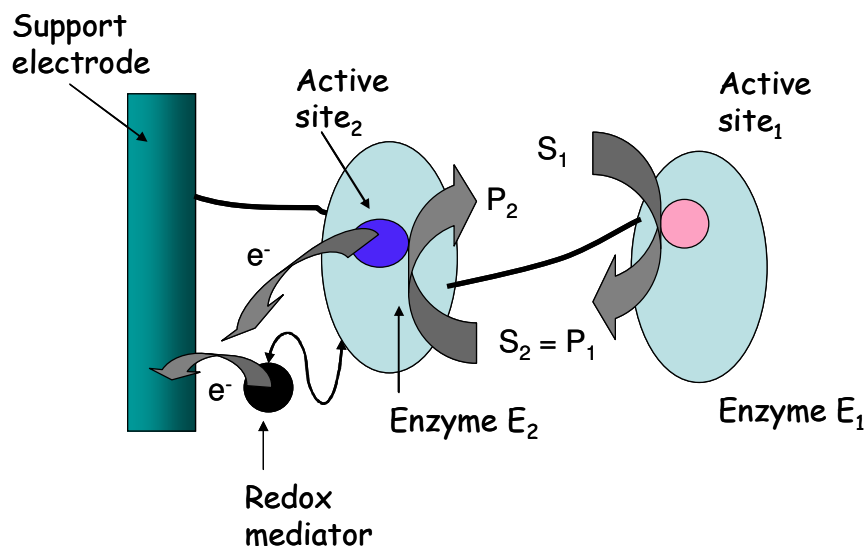


**Figure 10.** Enzyme amplification via coupling of two different enzymes.

### 3. MONOLAYER PROTECTED METALLIC NANOPARTICLE CLUSTERS (MPNC)

Although colloidal solutions of metals have been known for a long time, and a large variety of preparative techniques are now available, it is accepted that depending on the preparation conditions, nanoparticles exhibit a tendency to agglomerate slowly, and eventually lose their disperse character and flocculate. Furthermore the removal of the solvent generally leads to the complete loss of the ability to reform a colloidal solution.

These limitations have mainly been overcome since the realization in 1994 that alkane thiolate chains can adsorb onto gold nanoparticles to form monolayer protected gold nanoclusters. The reactivity of these 3D molecules is quite different from that of planar 2D SAMs attached to planar gold substrates. Because of the curvature of the gold core (see figure 11), the chain density of the alkane thiol monolayer decreases as the chain radiates from the core. The surface coordination of thiol molecules on finite metal crystallites can differ from that on bulk surfaces, depending on cluster size and geometry. For example the MPNC ligand coverage is in the range of 50% or more which is larger than the 33% (ligand/surface Au atom) coverage characteristic of 2D SAM on Au(111) faces.

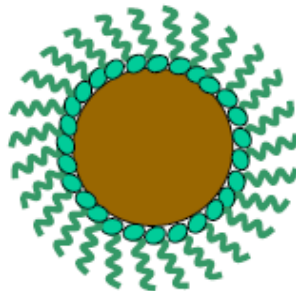


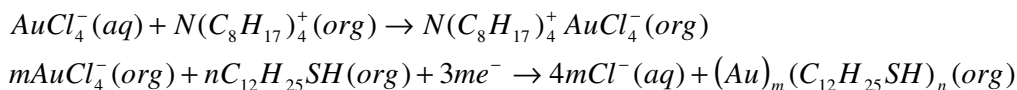
**Figure 11.** Schematic representation of metal nanoparticle with an adsorbed self assembled monolayer.

Monolayer protected metallic nanoparticle clusters (MPNC) have been intensively studied over the last decade. Why have such materials attracted such intense attention by so many workers? One reason is the well established fact that the catalytic properties of solids change with size. In many cases the catalytic activity increases as the size of catalyst particle approaches the nanoscale [26]<sup>4</sup>. In particular, alkane thiol based MPNC systems are of significant topical interest since they provide some of the building blocks of 'bottom up' engineered nanodevices and components and exhibit excellent potential as catalytic materials because of the large surface to volume ratio. Furthermore MPNC systems based on gold and silver atom clusters exhibit novel size dependent electronic properties such as quantized single electron charging [27]. Hence MPNC show a single electron transfer behaviour (the Coulomb Blockade) where electrons can tunnel through the ligand shell, thereby changing the charge state of the metal core. Charge transfer is only possible when certain core potentials are reached and the result is a staircase like current-potential response of current steps the magnitude of which depends on the value of the core potential.

The two phase methodology developed by Brust and Schiffrin [28]<sup>5</sup> (see fig.12) is often used to form relatively monodisperse alkanethiolate protected gold and silver nanoclusters with diameters less than 3 nm. The strategy involves using a two phase water/toluene system a reducible metal salt and a phase transfer agent to effect growth of metallic clusters with the simultaneous attachment of self assembled thiol monolayers on the growing nuclei. The reaction scheme involves, for example, the transfer of  $\text{AuCl}_4^-$  from aqueous solution to toluene using tetraoctylammonium bromide as phase transfer agent. Subsequently dodecanethiol is added to the organic phase  $\text{AuCl}_4^-$  to form a polymeric gold-thiol complex. Finally the latter is reduced by reaction with aqueous  $\text{BH}_4^-$  ion to form the thiol protected metal nanocluster. The sequence of events may be represented as follows (see fig.12(a) above as well):

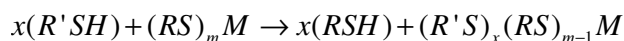
<sup>4</sup> Gold is very chemically inert and resistant to oxidation. However gold nanoparticles supported on  $\text{Co}_3\text{O}_4$ ,  $\text{Fe}_2\text{O}_3$  or  $\text{TiO}_2$  are highly active catalysts under high dispersion for CO and  $\text{H}_2$  oxidation, NO reduction, the water gas shift reaction,  $\text{CO}_2$  hydrogenation and the catalytic combustion of methanol.

<sup>5</sup> It should be noted that preparation of colloidal metals in a two phase system was introduced long ago by Faraday who reduced an aqueous gold salt with phosphorous in carbon disulfide and obtained a ruby coloured aqueous solution of dispersed gold particles.



Note that the source of electrons is the  $BH_4^-$  moiety. The conditions of the reaction determine the ratio of thiol to gold, i.e. the ratio  $n/m$ . Usually a 1:1 thiol gold ratio is used. However the latter can be varied and it has been established that larger ratios give smaller MPC core sizes, whereas fast reductant addition and cooled solutions produce smaller, more monodisperse MPNC's. Quenching the reaction immediately after reduction produces higher abundances of very small core sizes (typically  $\leq 2\text{ nm}$ ). An unusual property of these thiol derivitized metal nanoparticles is that they can be handled and characterized as a simple chemical compound. The dry product is dark brown, has a waxy texture and is soluble in non-polar solvents such as toluene, pentane and chloroform. Subsequent work has indicated that a wide range of alkanethiolate chainlengths (C3-C24),  $\omega$ -functionalised alkanethiolates and dialkyl disulfides can be employed using the basic Brust-Schiffrin protocol.

A particularly useful point to note is that the Brust-Schiffrin process tolerates considerable modification with respect to protecting ligand structure, and the core metal can be varied. Monolayer protected nanoclusters can be modified by replacing ligands using a place exchange protocol. For example MPNCs with alkanethiolate monolayers RS can be functionalised with R'S groups by the following place exchange reaction:



where M is the metal core, x and m are the stoichiometric numbers of new and original ligands respectively, may be conveniently followed using nmr analysis. The kinetics and thermodynamics of the latter reaction are controlled by factors such as the feed mole ratio of R'SH to RS, their relative steric bulk, and R versus R' chainlengths. The process generates mixed thiol capping shells containing a controlled mole fraction of alkane thiol units which may act as chemical receptors/hosts, or exhibit redox and/or catalytic activity.

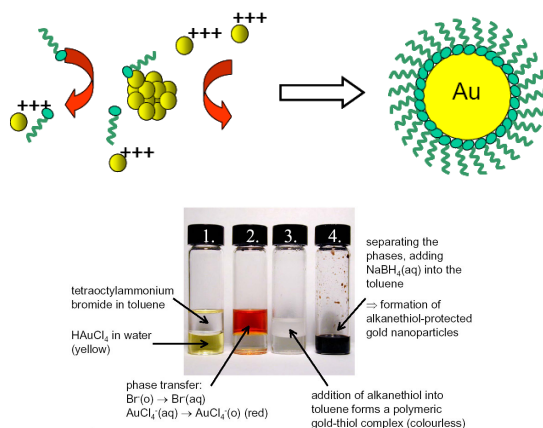


**Figure 12.** Schematic representation of Brust-Schiffrin method for MPNC fabrication.

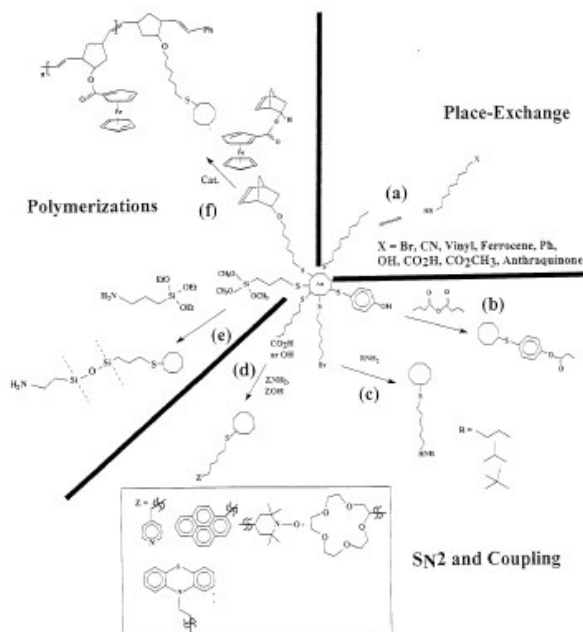


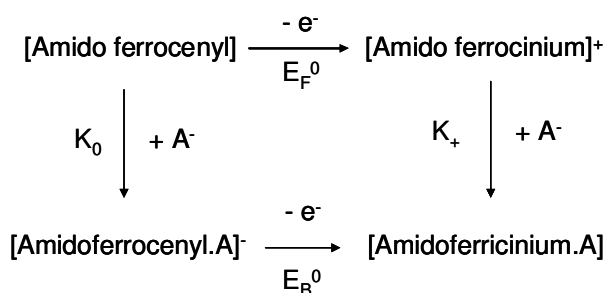
**Figure 13.** Reactions on MPNCs. (a) Place exchange, (b) reaction of p-mercaptophenol with propionic anhydride, (c)  $S_N2$  reaction of w-bromoalkanethiolated MPNCs with primary alkyl amines, (d) amide and ester coupling reactions, (e) siloxane formation reactions and (f) transition metal catalyzed ring opening metathesis polymerization (ROMP). [Adapted from ref.29].

As illustrated in fig.13 and discussed by Templeton and co-workers [29], functional groups on the outermost portion of the MPNC ligand sphere can undergo many synthetic transformations. The rich chemistry and synthetic possibilities have been discussed in a useful review by Templeton and co-workers [29]. For example  $S_N2$  reactions of mixed monolayer metal nanoclusters containing w-bromoalkanethiolates exhibit reactivities similar to those for primary halogen alkane monomers, but very different from analogous reactions on 2D SAMs.

The ability to modify the alkane thiol shell has an important significance with respect to chemical sensing and supramolecular chemistry [30-33]. Astruc and co-workers [30] have shown that gold nanoparticles capped with a shell containing a mixture of alkane thiol and amidoferrocenylalkylthiol (AFAT) ligands can be used as exo-receptors to detect anions in solution. The alkane thiols are made redox active via the presence of the amidoferrocene linkage and so the redox chemistry of the ferrocene group may be readily monitored via cyclic voltammetry. The titration of  $NBu_4^+$  salts of  $H_2PO_4^-$  and  $HSO_4^-$  with these functionalized (AFAT) coated gold nanoparticles can be monitored using cyclic voltammetry since the redox potential of the amidoferrocenyl group is sufficiently perturbed due to the interaction between the latter and the solution phase anion. The molecular interaction can be described as arising from a synergy between hydrogen bonding, electrostatic interaction and topology. The idea is illustrated schematically in figure 14. Addition of defined equivalents of the  $[n-Bu_4N][H_2PO_4]$  salt to a  $CH_2Cl_2$  solution of gold nanoparticles protected by a AFAT shell provokes the appearance of a new cathodically shifted wave whose current intensity

increases at the expense of the initial wave which describes the redox chemistry of the amidoferrocene/amidoferricenium redox couple. The replacement of the initial wave with the new one is essentially complete after addition of approximately 1 equivalent of [n-Bu<sub>4</sub>N][H<sub>2</sub>PO<sub>4</sub>]/amidoferricenyl branch, which implies that a one to one interaction between the anion and the amidoferricenyl group is operating (see fig.15(D)). The interaction process between the amidoferricenium group and the H<sub>2</sub>PO<sub>4</sub><sup>-</sup> anion can be described in terms of a square scheme with strong interaction in the Echegoyen-Kaifer model [34]<sup>6</sup>. The difference in potential between the initial uncomplexed wave and the complexed wave is large (typically some 220 mV) and provides access to the ratio of apparent association constants between the gold nanoparticle and the anion in the ferrocenyl (K<sub>0</sub>) and ferricenium (K<sub>+</sub>) forms.

In this model the interaction of the host is strong in one of the redox forms and weaker (but still significant) in the other. The ratio of apparent association constants is given by  $K_+/K_0 = \exp\left[\frac{nF}{RT}(E_F^0 - E_B^0)\right]$ . For example it has been shown that the apparent association constant K<sub>+</sub> between H<sub>2</sub>PO<sub>4</sub><sup>-</sup> ion and the amidoferricenium form of the gold nanoparticles is some 6210 times greater than that relating to the interaction between the anion and the amidoferricenyl form. The fact that the interaction of H<sub>2</sub>PO<sub>4</sub><sup>-</sup> ion is so much stronger with the amidoferricenium form than with the amidoferricenyl form signifies that the hydrogen bonding between the negatively charged oxygen of this anion and the positively charged NH group is the dominant one (refer to scheme 1 below). In contrast the recognition of HSO<sub>4</sub><sup>-</sup> corresponds to a square scheme with weak interaction in the Echegoyen-Kaifer model (K<sub>0</sub> << 1), whereby there is no new ferrocenyl wave observed on addition of the salt, but only a cathodic shift in the position of the original wave.



**Scheme 1.** Square scheme for amidoferricenyl redox chemistry and anion binding.

<sup>6</sup> In the Echegoyen-Kaifer model switching between binding states can be classified broadly into two categories, binary and incremental. The binary case refers to the situation in which there is no affinity between the anion and the neutral ligand, but an interaction occurs when the ligand is oxidised. The incremental case refers to all situations in which a finite binding interaction is observed between anion and ligand and this interaction strengthens upon oxidation of the ligand. Incremental behaviour is more suitable for rapid interconversions of molecular structure due to kinetic availability of the bound species in both binding states. Conversely, in the binary case, the off or zero state corresponds to an unbound state so that the rate of switching is, at best, limited by diffusion.

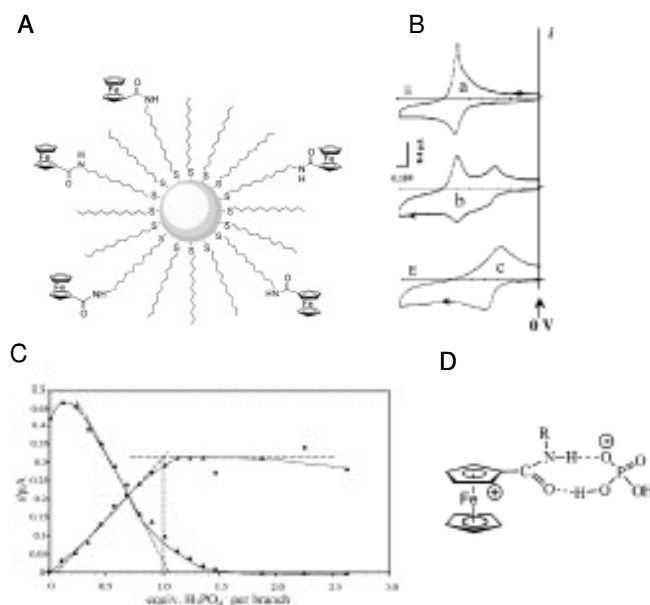


**Figure 14.** (A) Functionalised gold nanoparticles containing mixed thiol monolayer containing amidoferrocenyl thiol as diluent (29% doping). (B) Cyclic voltammetry of redox labeled gold nanoparticles in CH<sub>2</sub>Cl<sub>2</sub> solvent with 0.1 M n-Bu<sub>4</sub>NPF<sub>6</sub> supporting electrolyte. Pt electrode, sweep rate 200 mV/s. (a) without [n-Bu<sub>4</sub>N][H<sub>2</sub>PO<sub>4</sub>]; (b) 0.6 equivalents [n-Bu<sub>4</sub>N][H<sub>2</sub>PO<sub>4</sub>]/amidoferrocenyl branch; (c) excess [n-Bu<sub>4</sub>N][H<sub>2</sub>PO<sub>4</sub>]. (C) Titration of [n-Bu<sub>4</sub>N][H<sub>2</sub>PO<sub>4</sub>] with the 20-Fc AFAT gold nanoparticles as monitored by CV. The decrease in current intensity of the initial CV wave (triangles) and the increase in intensity of the new CV peak (circles) is shown as a function of the number of equivalents of H<sub>2</sub>PO<sub>4</sub><sup>-</sup> added per AFAT branch. (D) Schematic of double hydrogen bonding interaction between amidoferrocenium and H<sub>2</sub>PO<sub>4</sub><sup>-</sup> ion.

In recent work reported by Chen and co-workers [35] it has been shown that alkanethiol capped gold nanoclusters may be immobilized in a controlled manner on support electrode surfaces to form organized architectures of nanoparticles. This offers the possibility for the construction of a wide range of functionalized nanoparticle modified electrodes. Chen and co-workers utilized alkanedithiols as bifunctional linkers. The latter were incorporated into a previously prepared alkane thiol monolayer protected gold nanocluster of defined size using ligand place exchange methodology. The resulting particles were surface active with free thiol moieties present on the outer peripheral surface (see figure 15 (A)). Excess dithiol and displaced thiol molecules can subsequently be removed by liquid extraction from the exchange solution. Finally a planar 2D self assembled monolayer can be formed by immersing a gold substrate surface into the functionalized surface active nanoparticle solution. Surface modification of the gold follows via the usual adsorption and self assembly pathway. The ability to fabricate multilayer nanoparticle assemblies follows by repeating the fabrication protocol a number of times.

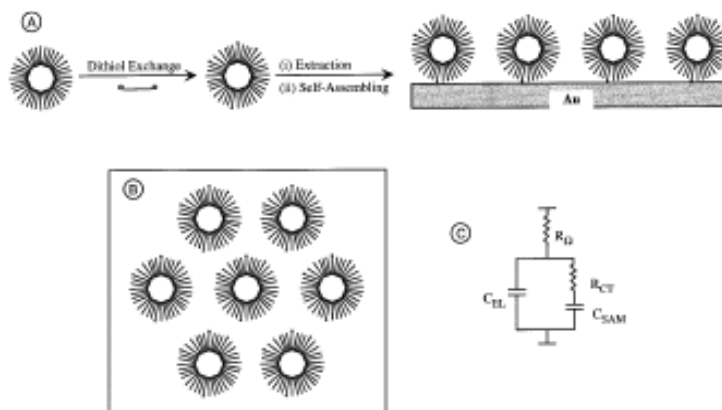


**Figure 15.** (A) Schematic of self assembly of surface active MPNC's. (B) Hypothetical surface structure of the adsorbed MPNCs. (C) Randles equivalent circuit for the MPNC surface assembly. In the latter  $R_{\Omega}$  denotes the uncompensated solution resistance,  $R_{CT}$  is the charge transfer or Faradaic resistance, and  $C_{SAM}$ ,  $C_{EL}$  reflect the components of the interfacial capacitance from the electrode surface with and without adsorbed MPNC species respectively.

The redox characteristics of the surface immobilized nanoparticle assembly can be probed using a variety of electrochemical techniques such as cyclic voltammetry and complex impedance spectroscopy. The Laviron theory of surface redox processes [23] may be used to estimate the surface electron transfer rate constant for the nanoparticle charging reaction ( $MPNC^z/MPNC^{z+1}$  process)<sup>7</sup>. Alternatively the complex impedance response may yield the desired quantity (typically  $10\text{ s}^{-1}$ ) via  $k_{ET} = \frac{1}{2C_{SAM}R_{CT}}$ . The latter quantity corresponds to a particular valence state change of the monolayer

protected metal nanoparticle since the latter may exhibit a large number of discrete electron transfers involving multiple valence states [36]. Because of a combination of small metal core size (typically 3 nm or less) and hydrocarbon like dielectric coating (typically dielectric constant is 2-3), the capacitance  $C_{CLU}$  of a MPNC can exhibit sub attofarad values when studied in non-aqueous solution. Addition or removal of single electrons from such tiny capacitors produce potential changes which are significant and can be readily measured via voltammetric techniques since  $\Delta V = \frac{e}{C_{CLU}} \gg \frac{k_B T}{e}$ . Hence

<sup>7</sup> The surface immobilized nanoparticles exhibit reasonably well defined Coulomb staircase charging effects which are similar to those shown by the MPNCs dispersed in organic solvents which diffuse to, and react at, an unmodified gold electrode. Hence the rate constant extracted using Laviron theory, or indeed via analysis of the complex impedance response will reflect a particular charging event such as  $MPNC^z \rightarrow MPNC^{z-1} + e^-$ .

We have seen that the control of nanoparticle properties provides opportunities for the design of unique systems. Indeed, as noted in a recent review by Rotello and co-workers [6(d)] the ability to combine molecular functionality with the inherent properties of nanosized entities makes MPNC scaffolds important tools for the creation of complex functional devices. Indeed application of the concepts of supramolecular chemistry and molecular recognition to nanoparticles introduces a means of control over the assembly of these systems into extended morphologies, thereby enabling the design of elaborate nanocomposite structures.

#### 4. ELECTRON TRANSFER DYNAMICS IN INTEGRATED NANOTUBE-BIOMOLECULE HYBRID SYSTEMS

Electron transfer in biological systems is one of the leading areas in the biochemical and biophysical sciences [38,39], and in the past few years there has been considerable interest in the direct electron transfer between redox proteins and electrode surfaces. In an amperometric biosensor the redox state of the analyte or a correlated species in the course of a reaction sequence is altered. By regeneration of its initial redox state at an electrode surface which is poised to a suitable potential, a current through the electrode is generated which is used as the sensor signal. If a substrate is specifically oxidized or reduced in an enzymatically catalysed reaction using an oxidoreductase as biological recognition element, the significant decrease in activation energy which is imposed by the catalytic action of the redox enzyme is possible by either immediately storing the redox equivalents in an enzyme integrated prosthetic group (e.g. FAD, PQQ, haeme, transition metals) or by transfer of electrons between a suitable co-substrate (e.g. FMN, NAD<sup>+</sup>, NADP<sup>+</sup>) and the analyte within the active site of the enzyme. The enzyme has then to be regenerated by a final electron transfer between the co-factor/co-substrate and the surface of the amperometric electrode leading to the current flow which is measured and directly proportional to the substrate concentration.

We first discuss the structure of a typical redox enzyme such as glucose oxidase, since this will be pertinent to the vital problem of making the active site in the enzyme electronically communicate with the underlying electrode support surface. The latter process must be rapid if an efficient amperometric biosensor is to be developed. Glucose oxidase is a dimeric protein (Figure 16) with a molecular weight of 160 kDa, containing one tightly bound ( $K_a = 1 \times 10^{-10}$ ) flavin adenine dinucleotide (FAD) unit per monomer as cofactor (actually two FAD-sites per enzyme). The FAD is not covalently bound and can be released from the holo-protein following partial unfolding of the protein. The dimeric protein displays an ellipsoidal shape with a high content of secondary structure (28% helix, 18% sheet). The GOx (native dimer) dimensions are 70 Å x 55 Å x 80 Å. Each subunit is a compact spheroid with approximate dimensions 60 Å x 52 Å x 37 Å. The two isoalloxazine moieties are separated by a distance of about 40 Å. Useful information describing aspects of the tertiary structure of the enzyme are described on the web [50].

The FAD exhibits redox activity  $FAD + 2H^+ + 2e^- \rightarrow FADH_2$ . Glucose oxidase exhibits a very high degree of specificity for β-D-glucose. The catalytic reaction sequence is described via the

ping-pong mechanism illustrated in scheme 2. Clearly the  $\text{H}_2\text{O}_2$  generated as part of the enzymatic catalytic cycle may be electrochemically detected at an underlying electrode thus making amperometric detection of glucose possible by monitoring the flow of current. Although peroxide detection results in a current flow, it is not an optimum strategy for amperometric detection since the electrode needs to be poised at a high anodic potential, typically 0.8 V. Under such conditions many other biomolecules present in blood, such as ascorbate or uric acid, may also undergo direct oxidation at the electrode and contribute to the observed current flow. Hence the selectivity of the device is lowered. Note also that the minimum distance between the flavin group and the surface of the monomer is 13 Å. This implies that a significant tunneling barrier to electron transfer exists between the flavin group and the support electrode surface which can mitigate against the effective functioning of GOx in an amperometric biosensor device. Hence attention has focused on developing strategies which will both reduce the detection potential applied to the electrode during amperometric operating conditions and to optimize the electronic communication between enzyme active site and electrode. These strategies involve the concept of redox mediation and enzyme immobilization.



**Figure 16.** Schematic representation of the glucose oxidase enzyme outlining the overall dimeric double quasi-ellipsoidal structure and the location of the flavin redox active group within one of the ellipsoids.

The design of a redox enzyme has evolved to protect the redox state of the integrated co-factor thereby avoiding unwanted redox processes with free diffusing redox species or other redox proteins. Consequently, the efficient regeneration of the enzymes active site at the electrode surface, is the key for the construction and optimization of amperometric enzyme biosensor electrodes. This fact has serious implications on the design strategy. Major problems arise from the need to immobilize the redox enzyme on the electrode surface while concomitantly preserving the enzymatic catalytic activity. It is also not trivial to design efficient electron transfer pathways between the immobilized enzyme and the electrode surface. Furthermore the sensor architecture should facilitate mass production and miniaturization and minimize unspecific side reactions.

In the following paragraphs possibilities for the design of reagentless amperometric biosensors will be discussed based on selected immobilization technologies with a major focus on non-manual enzyme fixation concomitantly defining suitable electron transfer pathways. This technology will define a pathway for smart enzyme biosensor devices.

Various immobilization strategies have been adopted to fabricate enzyme electrodes for biosensor applications. These strategies have exhibited varying degrees of success, and in addition to considering the direct electron transfer between the redox protein and the electrode (fig.17(A)), many strategies suggest that electron transfer mediators have to be used to facilitate electronic communication between the active site of the protein and the underlying electrode (refer to figure 17(B)).

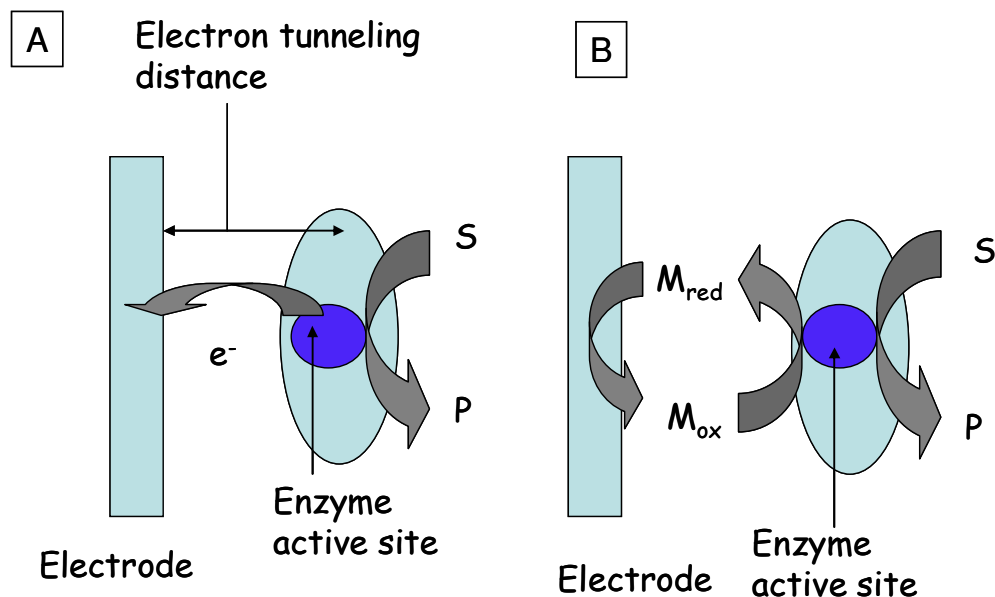


**Figure 17.** (A) Direct ET between active site of redox enzyme and support electrode. (B) Mediated ET involving soluble redox mediator small molecules and redox enzyme.

However the potential at which an amperometric enzyme biosensor is operated depends upon the redox potential of the mediator used rather than that exhibited by the active site of the redox enzyme. Usually the difference in magnitude between the latter potentials is significant (ca. 0.3 - 0.5 V) a factor which acts against successful biosensor operation, since the more positive the operating potential, the greater is the tendency for the sensor to respond to oxidizable substances present in the sample other than the target substrate.

Clearly the best strategy for successful enzyme biosensor<sup>8</sup> fabrication is to devise a configuration by which electrons can directly transfer from the redox center of the enzyme to the underlying electrode. This has been accomplished in recent years [40] using the idea of molecular wiring. Hence the enzyme can be modified with electron relays, through modification of the peripheral oligosaccharide with relay species pendant on the termini of flexible spacer chains, and indeed through relays in electron conducting hydrogels within which enzymes are covalently bound [41].

<sup>8</sup> The most widely used enzymes in biosensor systems are  $O_2$  dependent oxidases,  $NAD^+$  dependent dehydrogenases, PQQ dependent dehydrogenases and multi-cofactor enzymes containing a primary redox site (FAD,PQQ) internally coupled with electron acceptors such as haeme species.

The development of the so called ‘electroenzyme’[42] has proved to be significant (fig.20). One possibility involves enzyme modification by covalently attaching redox centers to suitable binding sites at the protein. The binding takes place either at the outer protein shell via terminal side chains of the amino acids [43], at the inner surface of the protein preferentially in close proximity to the redox-active cofactor [44], or at the cofactor of the enzyme [45].

Since the discovery by Iijima [9] in 1993, carbon nanotubes (CNT) have attracted enormous international interest because of their unique structural, mechanical and electronic properties. The electrochemical properties of both multi (MWCNT) and single walled (SWCNT) carbon nanotubes have not been extensively examined to date, although these materials should serve as excellent candidates for nanoelectrodes and platforms for nanoelectrochemical cells and amperometric biosensor devices.

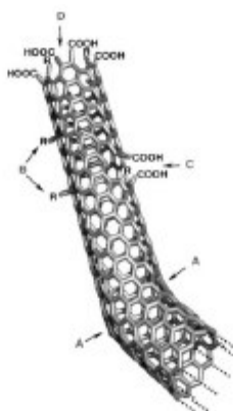


**Figure 18.** Typical defects found in a SWCNT. A: Five or seven membered rings in the carbon framework instead of the normal six membered ring. This leads to tube bending. B:  $sp^3$ -hybridized defects (R = H and OH). C: Carbon framework damaged by oxidative treatment which leaves a hole lined with COOH groups. D: open end of SWCNT terminated with COOH groups.

Carbon nanotubes can be regarded as  $sp^2$  carbon atoms arranged in grapheme sheets which have been rolled up to form a seamless hollow tube. The tubes are capped at the end by a fullerene type hemisphere and can have lengths ranging from tens of nanometers to several microns. The SWCNT variant used in the present research programme consists of a single hollow tube with diameters typically between 0.4 – 2 nm. The manner in which carbon nanotubes are prepared and treated before assembly on a support electrode surface will determine in no small way the subsequent performance of the nanotube modified electrode. In many cases the SWCNT are purified via treatment with strong mineral acids such as  $HNO_3$  or  $H_2SO_4$ . This treatment causes the reactive (compared with the sidewall) highly strained caps to be removed resulting in open ended tubes. The latter contain either dangling bonds when in contact with organic solvents which can undergo further chemical reaction or oxygenated functional groups such as quinones and carboxylic acids when the open ends are in contact with polar solvents. Note that the sidewalls also contain defect sites (as illustrated in fig.18) such as pentagon-heptagon pairs  $sp^3$  hybridized defects and lattice vacancies.

It should be noted that the ends of carbon nanotubes are quite hydrophilic since they are terminated in oxygenated species, but the sidewalls which comprise most of the tube surface are highly hydrophobic. This hydrophobicity presents a major challenge when it becomes necessary to disperse and manipulate the carbon nanotube for controlled assembly on electrode surfaces. The tubes exhibit a tendency to undergo rather rapid aggregation and coagulation when in contact with aqueous solution or polar solvents, although it is possible to extend the period over which the tubes remain in the dispersed state if they are first subjected to an acid shortening procedure. Hence the process of tube dispersion is usually performed in non polar organic solvents such as dimethylformamide (DMF) or with the aid of surfactants or polymer chains.

The integration of biomaterials (e.g. proteins/enzymes, antigens/antibodies, DNA) with CNT's provides new hybrid systems that combine the conductive or semiconductive properties of CNTs with the recognition and catalytic properties of the biomaterial. The latter synergy will yield new bioelectronic systems or templated nano-circuitry. The many applications of CNT-biomolecule hybrid systems have been recently comprehensively reviewed [10,46].

In a number of recent communications Lyons and co-workers [47-49] have demonstrated that glucose oxidase may be adsorbed on SWCNT mesh modified electrodes while still retaining a well defined redox activity and catalytic behaviour with respect to glucose oxidation. Typical AFM images of the SWCNT mesh both in the absence of and containing adsorbed glucose oxidase are presented in fig.19(a) and 19(b) respectively. The random and porous dispersed nature of the nanotube mesh is apparent from fig.19(a) and the high surface coverage of adsorbed redox enzyme is clear in fig.19(b). It was also shown that cyclic voltammetry could be used with profit to probe in real time the redox behaviour of the flavin group embedded within the protein sheath. The voltammograms presented in Fig. 20 were obtained using a bare, SWCNT-modified and SWCNT/GOx/Nafion-modified glassy carbon working electrodes in a 50 mM phosphate buffer (pH 7). As can be seen, while a bare GC electrode exhibits a virtually flat and featureless voltammetric response, a pair of well-defined redox peaks was observed at the SWCNT/GOx/Nafion-modified electrode. The observed peaks are characteristic of those representing the redox behaviour of an adsorbed species, in this case that of the flavin adenine dinucleotide FAD. The peaks are reasonably symmetrical and exhibit the characteristic bell shape expected for adsorbed redox species [50]. The absence of any peaks on the SWCNT-modified GC voltammogram suggests that the voltammetric response observed with the latter is essentially capacitive (at least in the potential window examined during the voltammetric sweep) in the absence of any redox active substrates present in the electrolyte solution. For the voltammetric response recorded for the SWCNT/GOx/Nafion composite electrode at a sweep rate of  $100 \text{ mVs}^{-1}$ , the cathodic peak potential ( $E_{pc}$ ) was  $-417 \text{ mV}$  vs. Ag/AgCl and the peak separation ( $\Delta E_p$ ) observed was  $41 \text{ mV}$ . The surface coverage of adsorbed redox enzyme was calculated by integrating the charge  $Q$  under the voltammetric peak using the formula:  $\Gamma = Q/nFA$  where  $A$  denotes the geometric electrode area,  $n$  denotes the number of electrons transferred in the redox process (2 in the present case) and  $F$  is the Faraday constant. Lyons et al.[47-49] estimated that  $\Gamma = 1.7 \text{ nmol cm}^{-2}$  for the Nafion coated SWCNT/GOx composite electrode.

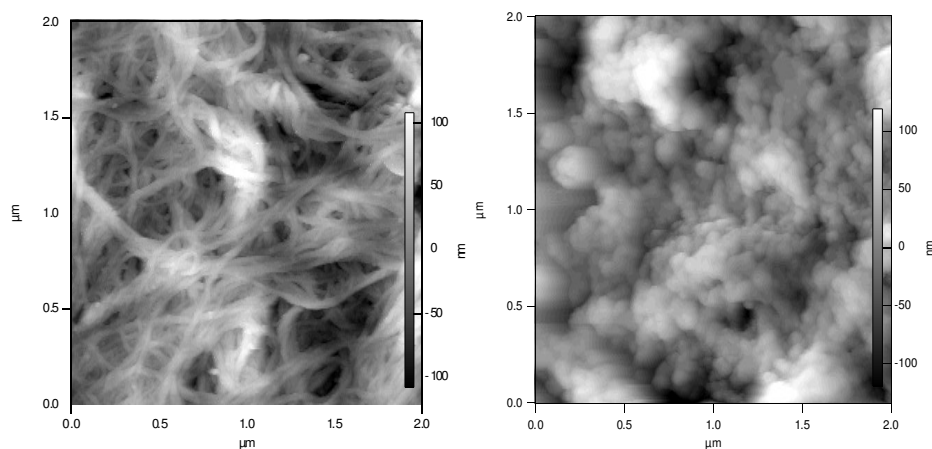


**Figure 19.** (a) AFM image recorded for ensemble of SWCNT dispersed randomly on a gold surface. (b) AFM image recorded for a SWCNT assembly dispersed randomly on a gold surface on which glucose oxidase was adsorbed for a 2.5 hr period at room temperature.

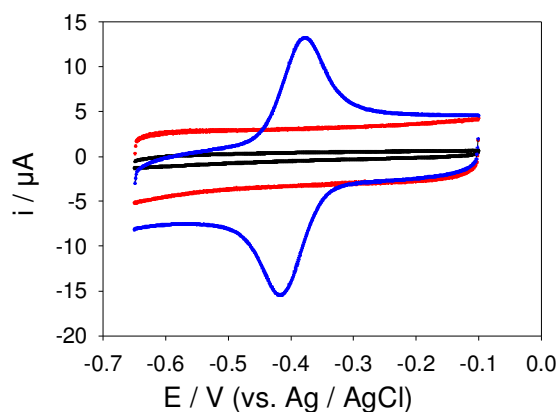


**Figure 20.** Cyclic voltammograms recorded at a bare (black), SWCNT-modified (red) and SWCNT/GOx/Nafion-modified (blue) glassy carbon working electrode. The electrolyte used in these experiments was a 50 mM phosphate buffer (pH 7) and the scan rate employed was  $100 \text{ mV s}^{-1}$ .

It is useful at this stage to comment on the nature of the interactions which result in enzyme immobilisation on the nanotube film, as the voltammetric data presented in fig.21 indicate that addition of a Nafion overcoating to the nanotube/GOx composite modified electrode enhances the redox activity of the latter and that the nanotube modified electrode is clearly superior to glassy carbon as an enzyme immobilisation platform. Wang *et al.* [51] have reported that glucose oxidase adsorbs preferentially to edge-plane sites on nanotubes. It has been established that such sites contain a significant amount of oxygenated functionalities. These groups are formed *via* the rupturing of carbon-carbon bonds at the nanotube ends and at defect sites which may occur on the side-walls. They render hydrophilicity and ionic character to the nanotubes and we believe that they are responsible for the ‘nesting’ of the protein on the nanotube film. The nanotubes and enzyme molecules are of similar

dimensions, which facilitates the adsorption of glucose oxidase without significant loss of its biocatalytic shape, form or function. We suggest that nanotubes can pierce the glycoprotein shell and gain access to the prosthetic group such that the electron tunneling distance is minimized. Such access is not generally possible with conventional 'smooth' electrodes, and significant unfolding of the protein shell can occur, resulting in the loss of biochemical activity.

Furthermore Wang and co-workers [51] have reported that SWCNT are readily solubilized in Nafion solutions made from ethanol or aqueous phosphate buffer. TEM images clearly indicate individual SWCNT ropes when dispersed in the latter media. This is in contrast to the high density intertwined aggregates found when SWCNT are dispersed in organic solvents such as chloroform. The structure of Nafion in solution may be viewed as a fluorocarbon backbone with protruding polar sulfonate  $\text{SO}_3^-$  groups. Hence it is similar in nature to other polymers which have been used to wrap and solubilise CNT material. According to Smalley and co-workers [52] the wrapping of nanotubes by water soluble polymers such as Nafion is a general phenomenon driven by a thermodynamic impetus to eliminate the hydrophobic interface between the tubes and the aqueous medium, thereby reducing the density of the tangled and rather dense tube assembly on the electrode surface. This may well increase the permeability of the void space between the tubes to increased quantities of electrolyte ions which will result in a change in the interfacial potential distribution and hence on the voltammetric response [53].

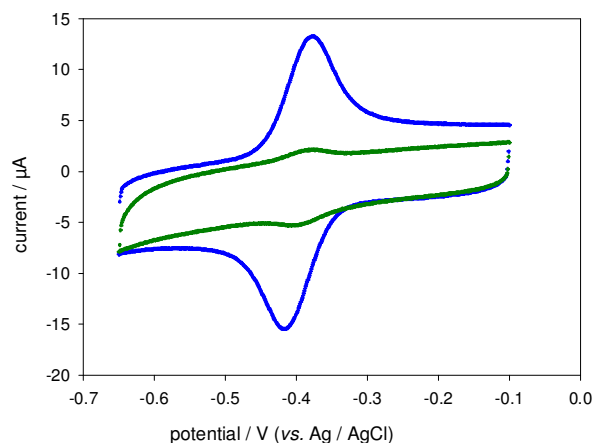


**Figure 21.** Cyclic voltammetric response of a GOx/Nafion modified glassy carbon electrode (green) and a SWCNT/GOx/Nafion modified glassy carbon electrode (blue). The protein film voltammetry was recorded in 50 mM phosphate buffer solution pH 7 at a sweep rate of  $100 \text{ mV s}^{-1}$ .

Ideally  $\Delta E_p$  should be zero for surface immobilized redox systems, [50]. The non zero  $\Delta E_p$  value observed in the voltammetric responses of the SWCNT/GOx modified electrode may be attributed to the presence of a potential difference between the electrode and the site of electron transfer (the flavin redox group) [54]. Such a difference would be attributed to the surrounding protein sheath acting as a dielectric layer. The presence of Nafion, while enhancing the discrimination between currents resulting from the surface redox reaction and that arising from the capacitive background contribution, may well result in a larger potential drop in the interface region. The prominent

background current is a consequence of the large, catalytically active surface area of the modified electrode [55,56].

The most important result obtained from the voltammetry data is the clear set of redox peaks obtained. Lyons and co-workers [47-49] that the latter are due directly to the direct electron transfer between the flavin prosthetic group embedded within the protein sheath and the underlying carbon nanotube strand. Hence we propose that the GOx molecules are adsorbed in a reasonably pristine configuration where the tunneling distance for electron transfer between the flavin sites and the nanotube strand is not too large hence making the transition probability for electron transfer favourable. It is important to note that the carbon nanotube and the enzyme molecule share a similar length scale and so the enzyme is able to adsorb on the nanotube sidewall without losing its biologically active shape, form and function. Indeed Baughman and co-workers [57] have introduced the striking analogy of piercing a balloon with a long sharp needle such that the balloon does not burst. Instead by a gentle twisting action the needle can be made to enter the balloon without catastrophe. Similarly it has been proposed [57] that some number of nanoscale 'dendrites' of CNT project outwards from the surface of a strand and act like bundled ultramicroelectrodes that are able to pierce the glycoprotein shell of glucose oxidase and gain access to the flavin prosthetic group such that the electron tunnelling distance is minimized and consequently electron transfer probability optimized. This degree of nanoscale electronic wiring and intimate access is not generally afforded with traditional smooth electrodes.

It could, of course, be suggested that the GOx species loses its flavin group on adsorption, and one may query whether the flavin moiety dissociates from the surrounding glycoprotein sheath when glucose oxidase is adsorbed on the surface of the nanotube. The flavin (either present in the solution or adsorbed on the nanotube surface) could then function as an inefficient redox mediator. In a recent paper Baughman and co-workers [57] examined the redox behaviour of both the free flavin molecule in the adsorbed state and when it is bound within glucose oxidase at single walled carbon nanotube modified electrodes using potential sweep voltammetry. The standard potential of the FAD/FADH<sub>2</sub> transition for both forms of flavin environment were similar, typically - 0.45 V vs Ag/AgCl (in good agreement with the data proposed by Lyons et al [47-49] ( $E^0 = - 0.396$  V see figure 20)) and so it is difficult to differentiate between adsorbed flavin and adsorbed protein bound flavin. Both forms give rise to characteristic bell shaped responses when subjected to a linear potential sweep. However if the flavin is free in solution then the voltammetric response observed should be quite different. A characteristic diffusive response is expected in the voltammogram. This is not observed in fig.20. Furthermore if the voltammetric response observed in figure 20 arose from ET activity associated with adsorbed free flavin molecules then one would expect that the voltammogram would be considerably distorted because of the fact that the electron would have to tunnel through a blocking layer of adsorbed holo-enzyme molecules which would also be present on the nanotube surface [58]. This distortion in the voltammetric profile is not observed.

The denaturation of glucose oxidase on a metal electrode surface has been experimentally examined using ellipsometry by Bockris and co-workers [58]. In this work two orientations of the enzyme molecule (shaped as a prolate ellipsoid with a major axis of 140 Å and minor axis of 50 Å) on the surface were observed: the major axis could be perpendicular to the surface (labelled the standing

position) or parallel to the surface (termed the lying position). It was determined that above a certain coverage enzymes in the standing position were not stable and undergo a transition to the lying position due to increasing intermolecular interaction. In the lying position the enzyme/substrate contact area is large and a gradual unfolding of the glycoprotein sheath occurs brought about largely by significant electrostrictive forces operating in the double layer region. The catalytic function of the enzyme is adversely effected because of this and eventually catalytic activity is lost. Hence a key determining factor in determining enzyme structural stability is the manner in which the enzyme is orientated with respect to the support electrode surface.

The recent work of Lyons et al [47] has clearly indicated that the nanotube assembly provides a matrix for the efficient immobilisation of a large loading of glucose oxidase and the Nafion binder/dispersal agent succeeds in preventing the loss of significant amounts of this enzyme to the solution during electrochemical experiments. It is also of interest to ask whether the redox enzyme maintains its innate catalytic activity when adsorbed on the sidewall of a carbon nanotube. Lyons et al. [49] have recently indicated that glucose oxidase maintains an excellent catalytic activity with respect to glucose oxidation when adsorbed on SWCNT strands immobilized on a support electrode surface in the form of a porous mesh. Indeed the glucose sensor can be operated at very low applied potential. In this work the amperometric response of a SWCNT/GOx/Nafion composite modified electrode to dissolved molecular oxygen under conditions of low potential in the presence of known concentrations of glucose in the solution was examined using slow sweep rate potential sweep voltammetry. The results of the latter experiments are presented in fig.22 and fig.23. In fig.22 the potentiodynamic response recorded for the electroreduction of molecular oxygen both in the absence and in the presence of glucose is illustrated. We note that the oxygen reduction current observed at the support electrode during the potential sweep *decreases* when glucose is added to the solution. In fig.23 the difference in oxygen reduction current (recorded at a fixed potential of  $-400$  mV) between that of a glucose free solution and one containing a finite quantity of glucose is plotted as a function of glucose concentration. An excellent linear relationship is obtained between the current decrease  $\Delta I$  and the glucose concentration. Hence glucose may be directly monitored in solution at an unprecedented low potential.

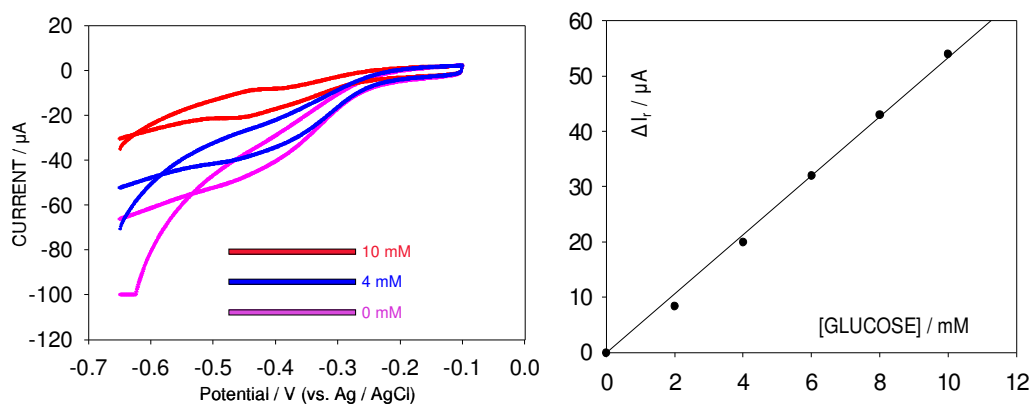


**Figure 22.** (a) Voltammetric response of SWCNT/GOx/Nafion composite electrode to glucose solutions saturated with oxygen. (b) Current-concentration response for oxygen reduction at a SWCNT/GOx/Nafion modified electrode in the presence of glucose.

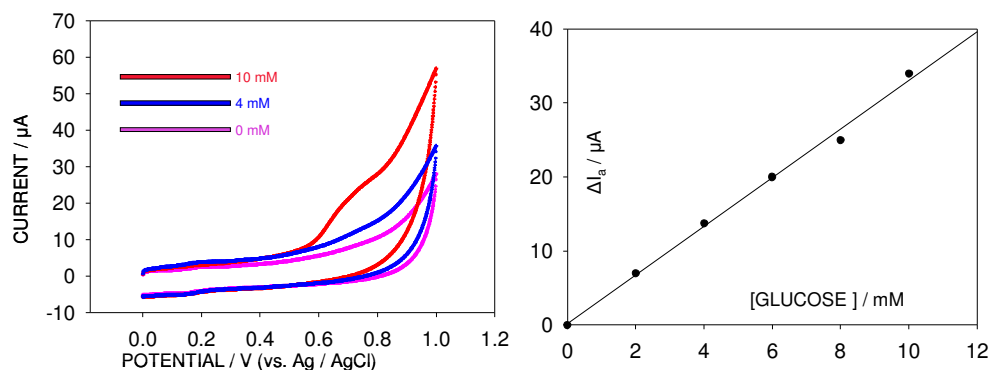


**Figure 23.** (a) Voltammetric response of SWCNT/GOx/Nafion composite electrodes in contact with oxygen saturated solution to glucose at high potential. (b) Calibration curve recorded at 0.9 V for glucose detection at a SWCNT/GOx/Nafion composite electrode.

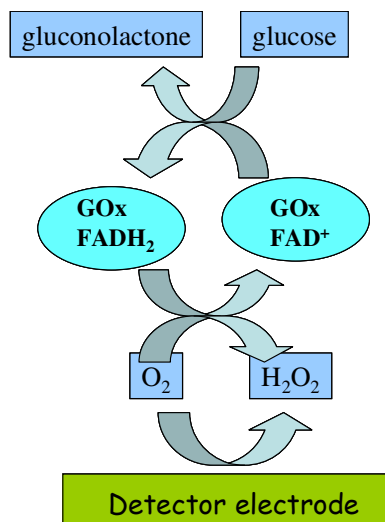
These observations may be understood by referring to the ‘ping-pong’ mechanistic scheme provided in scheme 2 where a competition exists between the direct reduction of molecular oxygen at the detector electrode and the reduction of di-oxygen in the reaction layer via reaction with the reduced glucose oxidase. It is clear that increasing the glucose concentration will reduce the concentration of free dioxygen at the interface and thereby result in a drop in the amperometric current response observed.

This result is significant from the perspective of the development of amperometric enzyme biosensors which will operate at low detection potential. It means that the natural co-factor for glucose oxidase may be effectively used under detection conditions where the oxidation of well known interferents such as ascorbate and uric acid does not occur. We can also infer from this result that the reduction of molecular oxygen at the dispersed SWCNT surface is relatively efficient due to the catalytic properties of the nanotube material. The question of the mechanism of catalysis remains open at the present time. It is tempting to suggest that active quinonoid groups on the nanotube surface may well enhance the electroreduction of molecular oxygen via a mediated catalytic mechanism.

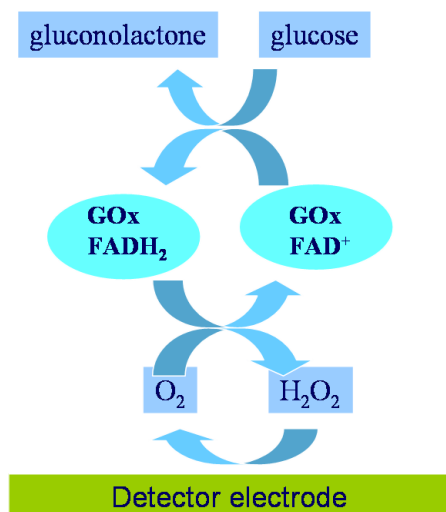
Lyons et al [49] have also shown (fig.23) that the composite electrode may be used at more elevated potentials, typically 0.9 V. In this case the amperometric current response (arising from the oxidation of the hydrogen peroxide generated via oxidised enzyme regeneration, is seen to increase in direct proportion to increasing glucose concentration. This detection mechanism (outlined in scheme 3 below) has been established for many years, but has been shown to be prone to interference by oxidizable components in solution.

The transport and kinetics of SWCNT modified electrodes has been recently subjected to a comprehensive theoretical evaluation by Lyons [59]. A mathematical model describing transport and kinetics of substrate and redox mediator within chemically modified electrodes comprising of redox enzymes immobilized in dispersed carbon nanotube meshes dispersed on support electrode surfaces was described. Two modes of amperometric detection were subjected to analysis. In the first the

current arising from re-oxidation of the reduced mediator at the support electrode is measured, whereas in the second the current arising from reduction of the oxidized mediator at the support surface is determined. Approximate analytical expressions for the substrate reaction flux within the nanotube layer are developed and related to the measured flux at the support surface. The kinetics both of substrate and mediator within the layer are also represented in terms of a kinetic case diagram.



**Scheme 2.** Ping Pong mechanism for glucose oxidation via the cyclic redox transformation of glucose oxidase (GOx.) using molecular oxygen as co-factor. Novel low potential amperometric detection via measurement of current arising from oxygen electroreduction at nanotube surface.



**Scheme 3.** Traditional high potential amperometric glucose detection via oxidation of hydrogen peroxide at underlying nanotube surface .

Recent work [60] has indicated that the chemical modification of electrode surfaces with carbon nanotubes<sup>9</sup> has enhanced the activity of the electrode with respect to the catalysis of biologically active species such as hydrogen peroxide, dopamine and NADH. Furthermore Multiwalled carbon nanotubes (MWCNT) have exhibited [60] good electronic communication with redox proteins where not only the redox centre is close to the protein surface such as in cytochrome c, azurin and horseradish peroxidase, but also when it is embedded deep within the glycoprotein such as in glucose oxidase (GOx).

An effective strategy, recently reported by Gooding and co-workers [61,62] and others [63] is to covalently attach an oxidatively shortened and functionalised SWCNT to an electrode (which has been previously chemically modified with a self assembled monolayer) and to subsequently covalently attach a redox active biomolecule to the head terminal of the aligned SWCNT using well established coupling chemistry, as illustrated in fig.24 and in scheme 4 below. Single walled nanotubes can be shortened in a 3:1 mixture of concentrated sulfuric and nitric acid. The oxidative shortening leaves several carboxylic acid groups at each end of the tubes. The latter can be converted to carbodiimide leaving groups using dicyclohexylcarbodiimide (DCC) which allows reaction with amine functionalities on cysteamine ( $\text{NH}_2(\text{CH}_2)_2\text{SH}$ ). The resultant tubes have thiol groups at each end which enable self assembly onto gold support surfaces to form well defined oriented arrays as evidenced from AFM analysis.

Using this methodology the spatial relation between the active site of the redox biomolecule with respect to the electrode is defined, the length of the tube can be controlled (via the duration of the oxidative shortening procedure), and the aligned SWCNT acts as an effective nanocontact. Very recently [62] the influence of the length of the carbon chain of a self assembled monolayer on gold electrodes on the electrochemical performance of carbon nanotube arrays attached to the SAM has been explored. Ruthenium hexamine in solution was used as a probe redox couple. The electrochemistry of the latter couple was found to decay exponentially with increasing methylene chain length as expected for a process controlled by quantum mechanical tunneling through an insulating barrier, rather than be attributed to diffusion through defects in the passivating SAM layer.

In further recent work Willner and co-workers[63] have prepared modified electrode surfaces comprising of oxidatively shortened SWCNT arrays oriented normal to electrode surfaces. The latter are formed via covalent linkage to cystamine units in mixed thiol monolayers deposited via self assembly on gold surfaces. The carboxylate group (formed as previously noted via oxidative shortening with aqueous acid) located on the free end of the oriented SWCNT may then be covalently coupled with an amino-derivative of the co-factor FAD to form an immobilized FAD modified SWCNT (surface coverage typically  $1.5 \times 10^{-10} \text{ mol cm}^{-2}$ ) which exhibits redox activity at a potential of  $-450 \text{ mV}$  (vs SCE), a value close to the thermodynamic redox potential of the FAD/FADH<sub>2</sub> redox couple. Apo-glucose oxidase can subsequently be re-constituted on the FAD units linked to the ends of the oriented SWCNT 'wires'. AFM analysis of the latter indicate that the surface is covered with densely packed clumps with an average lateral dimension of ca. 5 nm which can be reasonably

---

<sup>9</sup> Proteins and oligonucleotides can be non-specifically adsorbed on the external walls of CNTs .

attributed to individual GOx molecules associated with the FAD functionalized SWCNT. Typically the GOx surface coverage was estimated via EQCM analysis to be  $10^{-12}$  mol  $\text{cm}^{-2}$ . Typically the turnover rate of electrons to the electrode was estimated as  $4100 \text{ s}^{-1}$  which is about six times higher than the turnover rate of electrons from the active site of the native GOx to its natural acceptor ( $\text{O}_2$ ) which is typically some  $700 \text{ s}^{-1}$ . A clear quasi-linear correlation between turnover rate and the length of the SWCNT molecular wire was established. Thus the electron transfer barrier between the FAD center and the support electrode is lower for systems which use shorter SWCNT connectors. These results imply that electrons may be transported along SWCNT wires over distances as long as 220 nm. These distances clearly eliminate the possibility of charge transport via a tunneling mechanism.

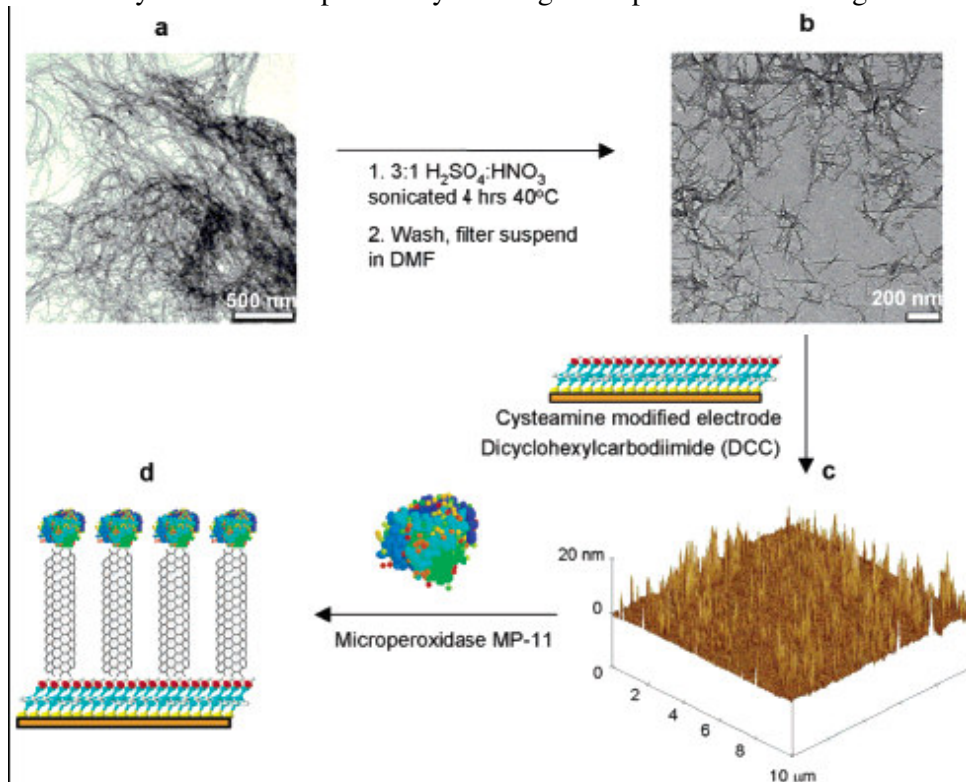
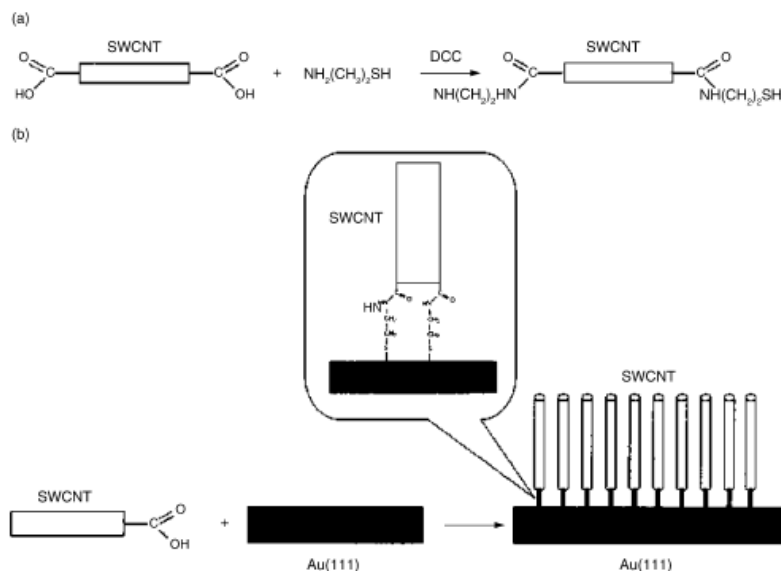


**Figure 24.** Schematic representation of the steps involved in the fabrication of aligned shortened SWCNT arrays for direct electron transfer with enzymes.

A possible origin for the length dependent electrical communication between the enzyme active site and the electrode may well involve the presence of defect sites located on the nanotube walls which were introduced during the oxidative shortening procedure. These sites act as local barriers to charge transport. The back-scattering of transported electrons from the defect sites to alternative fully conjugated charge transport paths or electron hopping over these defect sites may well explain the length dependence on electron turnover rate. Theoretical studies have predicted that a backscattering mechanism would reveal a charge transport rate that relates inversely to the length of the carbon nanotube due to the increase in the probability of defect sites as the CNTs are elongated.



**Scheme 4.** Schematic of the fabrication of aligned nanotube electrode arrays by self assembly.

The direct electrical contacting of redox enzymes and macroscopic electrodes by means of single walled carbon nanotubes represents a bridge between biosensor technology and nanotechnology. The field at set for considerable expansion in the short term and further rapid advances are to be expected.

## 5. CONCLUSIONS

In this review essay we have described some approaches which have been recently developed to fabricate smart nanostructures using a bottom up strategy based on materials science and electrochemistry. Many of these approaches have been interesting not only from a fundamental scientific viewpoint, but also pave the way forward for significant technological exploitation. The combination of biological molecules and novel nanomaterial components in new designed architectures is of considerable importance in the process of developing new nanoscale devices for future biological, medical and electronic applications. The successful development of specific methods which effectively expedite the electronic connection of redox active biomolecules to electrodes is presently one of the grand challenges in this field, and should be pursued vigorously if nanobiotechnology is to make the successful transition from promise to concrete reality.

## ACKNOWLEDGEMENTS

MEGL is grateful for the financial support of Enterprise Ireland, Grant Number SC/2003/0049, IRCSET Grant Number SC/2002/0169 and the HEA-PRTLTI Programme.

## References and Notes

1. Nanoscience and nanotechnologies: opportunities and uncertainties. The Royal Society and the Royal Academy of Engineering, London 2004. Report available free at the Royal Society's website at [www.royalsoc.ac.uk/policy](http://www.royalsoc.ac.uk/policy) and at The Royal Academy of Engineering's website at [www.raeng.org.uk](http://www.raeng.org.uk).
2. New dimensions for Manufacturing : A UK strategy for Nanotechnology. Department of Trade and Industry , London, June 2002. Available free of charge on the web at [www.dti.gov.uk/innovation/nanotechnologyreport.pdf](http://www.dti.gov.uk/innovation/nanotechnologyreport.pdf).
3. (a) Nanostructure science and technology. National Science Foundation, NSTC Report, WTEC, Loyola College, Maryland, 1999. Report available at [www.wtec.org/loyola/namo/](http://www.wtec.org/loyola/namo/). (b) Societal implications of nanoscience and nanotechnology. National Science Foundation, NSET Workshop Report, Arlington Va., March 2001. The report is located at [www.wtec.org/loyola/nano/societalimpact/nanosi.pdf](http://www.wtec.org/loyola/nano/societalimpact/nanosi.pdf).
4. (a) Nanotechnology Expert Group and Eurotech Data. Mapping excellence in nanotechnologies. Preparatory Study. European Commission, December 2001. The report is located at <http://europa.eu.int/comm/research/era/pdf/nanoexpertgroupreport.pdf>. (b) A position paper sponsored by the European Commission on the need for measurement and testing in nanotechnology is located at <http://europa.eu.int/comm/research/fp5/pdf/hleggrowth-nanotechnology.pdf>.
5. A useful bibliography of studies on nanoscience and nanotechnology from the philosophical, sociological and historical perspectives is available at [www.hyle.org/service/biblio/nano.htm](http://www.hyle.org/service/biblio/nano.htm).
6. For recent general reviews on metal nanoparticles see: (a) M-C. Daniel and D. Astruc, *Chem. Rev.* 104 (2004) 293 ; (b) A.C. Templeton, W.P. Wuelfing, and R.W. Murray, *Acc. Chem. Res.* 33(2000) 27. (c) A.N. Shipway, E. Katz and I. Wilner, *ChemPhysChem.*, 1(2000) 18 ; (d) U. Drechsler, B. Erdogan and V.M. Rotello, *Chem. Eur.J.*,10 (2004) 5570.
7. For recent papers illustrating the wide range of application areas served by nanostructured monolayers formed via adsorption/ self assembly see: (a) H.O. Finklea, *Electroanalytical Chemistry*; Marcel Dekker, New York, 19 (1996)19, 105. (b) J.J. Gooding, F. Mearns, W. Yang, J. Liu, *Electroanalysis*,15 (2003) 81 ; (c) F. Schreiber, *J. Phys.: Condens. Matter* , 16 (2004) R881.(d) J.H. Fendler, *Chem. Mater.*, 13 (2001) 3196. (e) J.C. Huie, *Smart Mater. Struct.*, 12 (2003) 264. (f) V. Chechik, C.J.M. Stirling, in *The chemistry of organic derivatives of Gold and Silver* (S. Patai and Z. Rappoport, eds.), Wiley, 1999, Chapter 15, pp.551-640.
8. (a) G.M. Wallraff, W.D. Hinsberg, *Chem. Rev.* 99 (1999)1801 ; (b) D.L. Feldheim, K.C. Grabar, M.J. Natan, T.E. Mallouk, *J. Am. Chem. Soc.*, 118 (1996), 7640; (c) A. Labande, J. Ruiz, D. Astruc, *J. Am. Chem. Soc.*, 124 (2002)1782.
9. (a) S. Iijima, *Nature*, 356 (1991) 56 ; (b) S. Iijima, *Nature* , 363 (1993) 603.
10. (a) J.J. Gooding, *Electrochim. Acta*, 50 (2005) 3049; (b) E. Katz, I. Willner, *ChemPhysChem.* 5 (2004)1084. (c) Y. Lin, S. Taylor, L. Huaping, K.A. Shiral Fernando, L. Qu, W. Wang, L. Gu, B. Zhou, Y.-P. Sun. *J. Mater. Chem.*, 14 (2004) 527.
11. (a) F.Ma, R.B. Lennox, *Langmuir*, 16 (2000) 6188 ; (b) E. Boubour, R.B. Lennox, *J. Phys. Chem. B.*, 104 (2000) 9004 ; (c) E. Boubour, R.B. Lennox, *Langmuir*, 16 (2000) 7464; (d) E. Boubour, R.B. Lennox, *Langmuir*, 16 (2000) 4222.
12. R.O'Brien and M.E.G. Lyons, Unpublished Ph.D work, University of Dublin, Trinity College, 2005.
13. R.O'Brien, M. Kinsella, Ph.D Thesis, University of Dublin 2006.
14. For a sample of recent work see: (a) A.W. Ghosh, T. Rakshit, S. Datta, *Nano Lett.*, 4 (2004) 565 ; (b) C.N. Lau, D.R. Stewart, S. Williams and M. Bockrath , *Nano Lett.*,4(2004) 569; (c) A. Troisi and M.A. Ratner, *Nano. Lett.*, 4 (2004) 591; (d) G. Maubach and W. Fritzsche, *Nano Lett.*, 4 (2004)

- 607; (e) K.K. Caswell, J.N. Wilson, U.H.F. Bunz and C.J. Murphy, *J. Am. Chem. Soc.*, 125 (2003) 13914. (f) W. Wang, T. Lee and M.A. Reed, *Rep. Prog. Phys.* 68 (2005) 523. (g) W. Wang, T. Lee and M.A. Reed, *Physica E*, 19 (2003) 117. (h) G. Maruccio, R. Cingolani, R. Rinaldi, *J. Mater. Chem.*, 14 (2004) 542.
15. For accounts of recent work on electron transmission through molecular wires and layers see: (a) A. Nitzan, *Annu. Rev. Phys. Chem.* 52 (2001) 681; (b) A. Nitzan and I. Benjamin, *Acc. Chem. Res.*, 32 (1999) 854; (c) A.W. Ghosh, P.S. Damle, S. Datta and A. Nitzan, *MRS Bulletin*, June 2004, 391; (d) G. Cuniberti, F. Grossmann and R. Gutierrez, *Adv. In Solid State Physics*, 42 (2002) 133; (e) A. Nitzan and M.A. Ratner, *Science*, 2003, 1384; (f) X.-Y. Zhu, *J.Phys. Chem.B.*, 108 (2004) 8778; (g) X.-Y. Zhu, *Surf. Sci. Rept.*, 56 (2004) 1; (h) D.M. Adams et al., *J.Phys. Chem.B.* 107 (2003) 6668.
16. For a selection of pertinent papers on long range electron transfer see: (a) C.E.D. Chidsey, C.R. Bertozzi, T.M. Putvinski and A.M. Mujscce, *J. Am. Chem. Soc.*, 112 (1990) 4301. (b) J.F. Smalley, S.W. Feldberg, C.E.D. Chidsey, M.R. Linford, M.D. Newton, Y-P Liu, *J. Phys. Chem.*, 99 (1995) 13141. (c) J.J. Sumner, K.S. Weber, L.A. Hockett and S.E. Creager, *J.Phys. Chem.B.*, 104 (2000) 7449; (d) J.F. Smalley, S.B. Sachs, C.E.D. Chidsey, S.P. Dudek, H.D. Sikes, S.E. Creager, C.J. Yu, S.W. Feldberg and M.D. Newton, *J. Am. Chem. Soc.*, 126 (2004) 14620.
17. (a) K. Habermuller, M. Mosbach and W. Schumann, *Fresenius J Anal. Chem.*, 366 (2000) 366, 560; (b) W. Schumann, *Rev. Mol. Biotechnol.*, 82 (2002) 425; (c) S. Sek, R. Bilewicz, *J. Electroanal. Chem.*, 509 (2001)11; (d) I. Willner, E. Katz, *Angew. Chem. Int.Ed.*, 39 (2000) 1180.
18. (a) J.J. Gooding, D. B. Hibbert, *Trends in Anal. Chem.*, 18 (1999) 525. (b) E.J. Calvo and A. Wolosiuk, *ChemPhysChem.*, 6 (2005) 43.
19. Recent work on nanobiotechnology is outlined in: (a) A.N. Shipway and I. Willner. *Acc. Chem. Res.*, 34 (2001) 421. (b) E. Katz and I. Willner, *ChemPhysChem.*, 5 (2004) 1084. (c) J.J. Gooding, *Electrochim. Acta*, 50 (2005) 3049. (d) Y. Lin, S. Taylor. H. Li, K.A. Shiral Fernando, L. Qu, W. Wang, L. Gu, B. Zhou, Y-P. Sun. *J. Mater. Chem.*, 14 (2004) 527. (e) E. Katz and I. Willner, *Angew. Chem. Int. Ed.* 43 (2004) 6042.
20. M.E.G. Lyons, *Electroactive Polymer Electrochemistry, Part 1*. Plenum Press New York, 1994. pp. 101-120.
21. For a selection of recent papers on the SAM/aqueous solution interface refer to: (a) C.P. Smith and H.S. White, *Langmuir*, 9 (1993)1; (b) C.P. Smith and H.S. White, *Anal. Chem.*, 64 (1992) 2396; (c) W. R. Fawcett, *J. Electroanal. Chem.*, 178 (1994)117; (d) I.M. Shiryayeva, J.P. Coleman, R. Boulatov and C.J. Sunderland, *Anal. Chem.*, 75 (2003)494; (e) S.E. Creager, G.K. Rowe, *J. Electroanal. Chem.*, 420 (1997) 291; (f) R. Andreu, J.J. Calvente, W.R. Fawcett, M. Molero, *J.Phys. Chem.B.*, 101 (1997) 2884 ; (g) J.J. Calvente, R. Andreu, M. Molero, G. Lopez-Perez, M. Dominguez, *J. Phys. Chem. B.*, 105 (2001) 9557.
22. Recent papers discussing electrolyte effects on the voltammetric response of SAMs include: (a) G.K. Rowe and S.E. Creager, *Langmuir*, 7 (1991) 2307 ; (b) K. Uosaki, Y. Sato, H. Kita, *Langmuir*, 7 (1991) 1510 ; (c) K.S. Weber, S.E. Creager, *J. Electroanal. Chem.*, 458 (1998)17; (d) H.O. Finklea, M.S. Ravenscroft, D.A. Snider, *Langmuir*, 9 (1993) 223.
23. Useful papers dealing with the theory of surface immobilized processes are: (a) E. Laviron, *J. Electroanal. Chem.*, 101 (1979) 19 ; (b) J.C. Myland, K. B. Oldham, *Electrochemistry Communications*, 7 (2005) 282 ; (c) M.J. Honeychurch, *Langmuir*, 15 (1999) 5158 ; (d) T.M. Nahir, E.F. Bowden, *J. Electroanal. Chem.*, 410 (1996) 9 ; (e) K. Weber and S.E. Creager, *Anal. Chem.*, 66 (1994) 3164 ; (f) L. Tender, M.T. Carter and R.W. Murray, *Anal. Chem.*, 66 (1994) 3173 ; (g) M.J. Honeychurch, G.A. Rechnitz, *Electroanalysis*, 10 (1998) 285 ; (h) M.J. Honeychurch, G.A. Rechnitz, *Electroanalysis*, 10 (1998) 453.
24. I. Willner, A. Riklin, B. Shoham, D. Rivenzon, E. Katz, *Adv. Mater.*, 5 (1993) 912.
25. A. Riklin, I. Willner, *Anal. Chem.*, 67 (1995) 4118.

26. (a) M. Moreno-Manas, R. Pleixats, *Acc. Chem. Res.* 36 (2003) 638; (b) R.M. Crooks, M. Zhao, L. Sun, V. Chechik, L.K. Yeung, *Acc. Chem. Res.* 34 (2001) 181; (c) S.E. Eklund, D.E. Cliffel, *Langmuir*, 20 (2004) 6012; (d) K. Judai, S. Abbet, A.S. Worz, U. Heiz, C.R. Henry, *J. Am. Chem. Soc.*, 126 (2004) 2732.
27. For a selection of recent literature on MPNC chemistry see: (a) B.M. Quinn, P. Lijeroth, V. Ruiz, T. Laaksonen, K. Kontturi, *J. Am. Chem. Soc.*, 125 (2003) 6644; (b) R.M. Lahtinen, S.F.L. Mertens, E. East, C.J. Kiely, D.J. Schiffrin, *Langmuir*, 20 (2004) 3289; (c) J.F. Hicks, D.T. Miles and R.W. Murray, *J. Am. Chem. Soc.*, 124 (2002) 13322; (d) S. Chen and R.W. Murray, *J. Phys. Chem. B.*, 103 (1999) 9996; (e) S. Chen, R.W. Murray, S.W. Feldberg, *J. Phys. Chem. B.*, 102 (1998) 9898.
28. (a) M. Brust, M. Walker, D. Bethell, D.J. Schiffrin and R. Whyman, *J. Chem. Soc., Chem. Commun.*, 1994, 801; (b) M. Brust, J. Fink, D. Bethell, D.J. Schiffrin and C. Kiely, *J. Chem. Soc. Chem. Commun.*, 1995, 1655; (c) D. Bethell, M. Brust, D.J. Schiffrin and C. Kiely, *J. Electroanal. Chem.*, 409 (1996) 137.
29. A.C. Templeton, W.P. Wuelfing and R.W. Murray, *Acc. Chem. Res.*, 33 (2000) 27.
30. (a) A. Labande and D. Astruc, *Chem. Commun.*, 2000, 1007; (b) A. Labande, J. Ruiz, D. Astruc, *J. Am. Chem. Soc.*, 124 (2002) 1782.
31. M-C. Daniel and D. Astruc, *Chem. Rev.*, 104 (2004) 293.
32. U. Drechsler, B. Erdogan, V.M. Rotello, *Chem. Eur. J.*, 10 (2004) 5570.
33. A.N. Shipway, E. Katz, I. Willner, *ChemPhysChem.*, 1 (2000) 18.
34. S.R. Miller, D.A. Gustowski, Z. Chen, G.W. Gokel, L. Echegoyen, A.E. Kaifer, *Anal. Chem.*, 60 (1988) 2021.
35. (a) S. Chen, R.W. Murray, *J. Phys. Chem. B.*, 103 (1999) 9996. (b) S. Chen, *J. Phys. Chem. B.*, 104 (2000) 663. (c) W. Song, M. Okamura, T. Kondo, K. Uosaki, *J. Electroanal. Chem.*, 554/555 (2003) 385. (d) M.G. Ancona, S.D. Jhaveri, D.A. Lowry, L.M. Tender, E.E. Foos, A.W. Snow, *Electrochim. Acta*, 48 (2003) 4157.
36. (a) B.M. Quinn, P. Liljeroth, V. Ruiz, T. Laaksonen, K. Kontturi, *J. Am. Chem. Soc.*, 125 (2003) 6644. (b) S. Chen, J.M. Sommers, *J. Phys. Chem. B.*, 105 (2001) 8816. (c) N.K. Chaki, B. Kakade, K.P. Vijayamohanan, *Electrochemistry Commun.*, 6 (2004) 661. (d) D.T. Miles and R.W. Murray, *Anal. Chem.*, 75 (2003) 1251. (e) J.F. Hicks, A.C. Templeton, S. Chen, K.M. Sheran, R. Jasti, R.W. Murray, J. Debord, T.G. Schaaf, R.L. Whetten, *Anal. Chem.*, 71 (1999) 3703. (f) S. Chen, R.S. Ingram, M.J. Hostetler, J.J. Pietron, R.W. Murray, T.G. Schaaf, J.T. Khoury, M.M. Alvarez, R.L. Whetten, *Science*, 280 (1998) 2098.
37. For a survey of pertinent theory refer to: (a) M.J. Weaver, X. Gao, *J. Phys. Chem.*, 97 (1993) 332. (b) J.R. Reimers, N.S. Hush, *J. Phys. Chem. B.*, 105 (2001) 8979. (c) S. Chen, R.W. Murray, S.W. Feldberg, *J. Phys. Chem. B.*, 102 (1998) 9898. (d) B. Su, H.H. Girault, *J. Phys. Chem. B.*, 109 (2005) 11427. (e) B. Su, H.H. Girault, *J. Phys. Chem. B.*, 109 (2005) 23925.
38. A.M. Kuznetsov and J. Ulstrup, *Electron transfer in chemistry and biology*. Wiley, New York, 1998.
39. *Electron transfer in Chemistry. Vol. 1: Principles, Theories, Methods and Techniques*. V. Balzani (Editor). Wiley-VCH, Weinheim, 2001.
40. (a) Y. Xiao, F. Patolsky, E. Katz, J.F. Hainfeld, I. Willner, *Science*, 299 (2003) 1877. (b) E.J. Calvo, A. Wolosiuk, *ChemPhysChem.*, 6 (2005) 43. (c) I. Willner, B. Willner, E. Katz, *Rev. Mol. Biotech.*, 82 (2002) 325. (d) B. Limoges, J.M. Saveant, D. Yazidi, *J. Am. Chem. Soc.*, 125 (2003) 9192. (e) M. Dequaire, B. Limoges, J. Moiroux, J.M. Saveant, *J. Am. Chem. Soc.*, 124 (2002) 240. (f) A. Anne, C. Demaille, J. Moiroux, *J. Am. Chem. Soc.*, 123 (2001) 4817. (g) N. Anicet, A. Anne, C. Bourdillon, C. Demaille, J. Moiroux, J.M. Saveant, *Faraday Discuss.*, 116 (2000) 269. (h) C. Bourdillon, C. Demaille, J. Moiroux, J.M. Saveant, *Acc. Chem. Res.*, 29 (1996) 529. (i) C. Bourdillon, C. Demaille, J. Moiroux, J.M. Saveant, *J. Am. Chem. Soc.*, 115 (1993) 2.

41. (a) W. Schuhmann, *Rev. Mol. Biotechnol.*, 82 (2002) 425. (b) K. Habermuller, M. Mosbach, W. Schuhmann, *Fresenius J Anal. Chem.*, 366 (2000) 560. (c) R.S. Freire, C.A. Pessoa, L.D. Mello, L.T. Kubota, *J. Braz. Chem. Soc.*, 14 (2003) 230.
42. A. Heller and Y. Degani, in *Redox Chemistry and Interfacial Behaviour of Biological Molecules*, G. Dryhurst, K. Nike (Eds), Plenum Publishing, New York, 1998, pp.151-171.
43. (a) W. Schuhmann, T.J. Ohara, H.L. Smith, A. Heller, *J. Am. Chem. Soc.*, 113 (1991) 1394. (b) A.D. Ryabov, A.M. Trushkin, L.I. Baksheeva, *Angew. Chem. Int. Ed. Engl.*, 31 (1992), 789. (c) H.L. Schmidt, F. Gutberlet, W. Schuhmann, *Sens. Actuat. B.*, 13-14(1993) 366. (d) W.C. Tsai, A.E.G. Cass, *Analyst*, 120 (1995) 2249.
44. (a) Y. Degani, A. Heller, *J. Phys. Chem.*, 91 (1987) 1285. (b) Y. Degani, A. Heller, *J. Am. Chem. Soc.*, 111 (1989) 2357. (c) P.N. Bartlett, R.G. Whitaker, M.J. Green, J.E. Frew, *Chem. Commun.*, 1987, 1603.
45. A. Riklin, E. Katz, I. Wilner, A. Stocker, A.F. Buckmann, *Nature*, 376 (1995) 672.
46. J.J. Davis, D.A. Morgan, C.L. Wrathmell, D.N. Axford, J. Zhao, N. Wang, *J. Mater. Chem.*, 15 (2005) 2160.
47. M.E.G. Lyons, G.P. Keeley, *Sensors*, 6 (2006) 1791.
48. M.E.G. Lyons, G.P. Keeley, *Int. J. Electrochem. Sci.*, 3(2008)819.
49. M. E. G Lyons, G. P. Keeley, *Chemical Communications*, 2008, pp.2529-2531.
50. E. Laviron, *J. Electroanal. Chem.* 101 (1979) 19.
51. (a) J.X. Wang, M. Musameh, Y. Lin, *J. Am. Chem. Soc.*, 123 (2003) 2408 ; (b) J. Wang, M. Musameh, *Anal. Chem.*, 75 (2003) 2075.
52. M.J. O'Connell, P. Boul, L.M. Ericson, C. Huffman, Y. Wang, E. Haroz, C. Kuper, J. Tour, K.D. Ausman, R.E. Smalley, *Chem. Phys. Lett.*, 342 (2001) 265.
53. (a) C.P. Smith, H.S. White, *Anal. Chem.*, 64 (1992) 2398. (b) M. Ohtani, S. Kuwabata, H. Yoneyama, *Anal. Chem.* 69 (1997) 1045. (c) A.P. Brown, F.C. Anson, *Anal. Chem.*, 49 (1977) 1589. (d) M.J. Honeychurch, G.A. Rechnitz, *Electroanalysis*. 10 (1998) 285. (e) M.J. Honeychurch, G.A. Rechnitz, *Electroanalysis*. 10 (1998) 453.
54. I.M. Shiryava, J.P. Collman, R. Boulatov, C.J. Sunderland, *Anal. Chem.*, 75 (2003) 494.
55. J. Li, A. Cassell, L. Delzeit, J. Han, M. Meyyappan, *J. Phys. Chem. B* 106 (2002) 9299.
56. L. Roullier, E. Laviron, *J. Electroanal. Chem.* 157 (1983) 193.
57. A. Guiseppi-Elie, C. Lei, R.H. Baughman, *Nanotechnology*, 13 (2002) 559.
58. A. Szucs, G.D. Hitchens, J.O'M. Bockris, *J. Electrochem. Soc.*, 136 (1989) 3748.
59. Michael E.G. Lyons, *Int. J. Electrochem. Sci.*, 4(2009) 77.
60. (a) G. Wang, J.J. Xu, H.Y. Chen, *Electrochem. Commun.*, 4 (2002) 506. (b) K. Yamamoto, G. Shi, T.S. Zhou, F. Xu, J.M. Xu, T. Kato, J.Y. Jin, L. Jin. *Analyst*, 128 (2003) 249. (c) J.J. Davis, K.S. Coleman, B.R. Azamian, C.B. Bagshaw, M.L.H. Green, *Chem. Eur. J.*, 9 (2003) 3732 ; (d) B.R. Azamian, K.S. Coleman, J.J. Davis, M.L.H. Green, *Chem. Commun.*, 2002, 366.
61. (a) J.J. Gooding, R. Wibowo, J. Li, W. Yang, D. Losic, S. Orbons, F.J. Mearns, J.G. Shapter, D. B. Hibbert. *J. Am. Chem. Soc.*, 125 (2003) 9006. (b) J.J. Gooding, *Electrochim. Acta.*, 50 (2005) 3049. (c) J. Liu, A. Chou, W. Rahmat, M.N. Paddon-Row, J.J. Gooding, *Electroanalysis*, 17 (2005) 38 .
62. A. Chou, P.K. Eggars, M.N. Paddon-Row, J.J. Gooding, *J. Phys. Chem. C.*, 113 (2009) 3203.
63. F. Patolsky, Y. Weizmann, I. Willner, *Angew. Chem. Int. Ed.* 43 (2004) 2113.